5-2013

Haldane pseudopotentials and Landau level mixing in the quantum Hall effect

Rachel Elizabeth Wooten
rwooten1@utk.edu

To the Graduate Council:

I am submitting herewith a dissertation written by Rachel Elizabeth Wooten entitled "Haldane pseudopotentials and Landau level mixing in the quantum Hall effect." I have examined the final electronic copy of this dissertation for form and content and recommend that it be accepted in partial fulfillment of the requirements for the degree of Doctor of Philosophy, with a major in Physics.

Joseph H. Macek, Major Professor

We have read this dissertation and recommend its acceptance:

John J. Quinn, Adriana Moreo, Janice L. Musfeldt, Predrag S. Krstić

Accepted for the Council:

Carolyn R. Hodges

Vice Provost and Dean of the Graduate School

(Original signatures are on file with official student records.)

5-2013

Haldane pseudopotentials and Landau level mixing in the quantum Hall effect

Rachel Elizabeth Wooten
rwooten1@utk.edu

To the Graduate Council:

I am submitting herewith a dissertation written by Rachel Elizabeth Wooten entitled "Haldane pseudopotentials and Landau level mixing in the quantum Hall effect." I have examined the final electronic copy of this dissertation for form and content and recommend that it be accepted in partial fulfillment of the requirements for the degree of Doctor of Philosophy, with a major in Physics.

Joseph H. Macek, John J. Quinn, Major Professor

We have read this dissertation and recommend its acceptance:

Adriana Moreo, Janice L. Musfeldt, Predrag S. Krstić

Accepted for the Council:
Carolyn R. Hodges

Vice Provost and Dean of the Graduate School

(Original signatures are on file with official student records.)

Haldane pseudopotentials and Landau level mixing in the quantum Hall effect

A Dissertation

Presented for the

Doctor of Philosophy

Degree

The University of Tennessee, Knoxville

Rachel Elizabeth Wooten

May 2013

Acknowledgements

I would never have been able to finish this dissertation without the help of Jack Dongarra, his group and especially Jakub Kurzak, the National Institute for Computational Sciences, my advisors Joseph Macek and John Quinn, and finally my friends and my family.

I would like to thank Jack Dongarra and Jakub Kurzak and the National Institute for Computational Sciences (NICS) for their advice and help in improving my numerical results.

And of course, I want to thank my advisors Joseph Macek and John Quinn. Thank you for encouraging me to study both analytic and numerical techniques to prepare me in my future and for all of the help working through my many, many questions. I am so glad to have had the opportunity to work with such dedicated, helpful, and supportive advisors.

I would also like to thank the other members of my committee, Predrag Krstic, Adriana Moreo, and Janice Musfeldt for taking the time to evaluate my research and studies.

I want to thank my friends, my younger sister, and my parents for always finding the time to encourage me and support me.

Abstract

The discovery of the quantum Hall effect in 1980 opened to physics one of the simplest systems for studying many-body correlations. Numerical techniques and trial wavefunctions have proven useful for describing the novel collective behavior of the electrons, but have not fully explained all features of the fractional quantum Hall effect. For example, it is predicted that Landau level mixing should have a moderate effect on the system for all but the very strongest magnetic fields, but this effect has not been extensively studied. Among the tools most useful to modeling and describing the quantum Hall system is the Haldane pseudopotential, which is the energy of electron pairs as a function of their coupled total angular momentum. Because the pseudopotential uniquely determines the correlative behaviors in the quantum Hall system, the study of the pseudopotential is particularly important. In this dissertation I will first derive novel analytic expressions for the pair interactions and the pseudopotential using the techniques of angular momentum algebra. Then, I will use these results to numerically determine the effect of Landau level mixing on the pair pseudopotentials.

Contents

Chapter 1

The quantum Hall effect

In recent decades, research into systems involving strongly correlated particles has increased tremendously in many fields, including atomic, nuclear, and solid state physics. A correlated system refers to any system where particle-particle interactions affect the behavior of the system as a whole and where these interactions cannot be ignored in any accurate model of the system. Although an exact description of correlated electrons is impossible for macroscopic systems, small systems are simple enough to allow exact numerical calculations of their spectra. In addition, the quantum Hall system is somewhat unique in that the aggregate behavior can be predicted based on modifications to the pair interactions. In this dissertation, I will derive an analytic formulation for describing the pair interactions, known as the pair pseudopotential, and will calculate how level mixing affects the pair interactions.

But before discussing my results, I will first discuss the physical system being modeled and its historical discovery.

1.1 Physical system

The quantum Hall system is a two-dimensional metal sheet with a strong magnetic field, $\mathbf{B} = B_z$, applied perpendicular to its surface. When a current flows along the surface, say in the x-direction, the magnetic force deflects it towards the edge of the

sheet. The charges build up at the edges until their electric field, E_y, produces a force on them that exactly balances the magnetic force, and all additional electrons continue undeflected in the x-direction. The Hall coefficient is defined as the ratio of the resulting electric field to the magnetic field times the current density, $R_H = E_y/B_z j_x$, once the system has reached equilibrium. In the classical Drude model, the Hall coefficient is a fundamental property of the metal [Ashcroft and Mermin (1976)] and provides a direct measurement of carrier charge and density. However, at low temperatures, the Hall coefficient is non-linear as a function of the magnetic field. At certain values of the magnetic field, the Hall coefficient levels off into plateaus, as seen in figure 1.1. In addition, the longitudinal resistivity, V_x/I_x, drops dramatically at these plateaus. The Hall coefficient is quantized as $R_H = \nu h/e^2$, where the filling factor, ν, takes on integer or rational fraction values. The integer quantum Hall effect (where ν is an integer), is so robust that the measured value of h/e^2 is used as the international standard unit of resistance [NIST (2005)] known as the von Klitzing constant, R_K, after Klaus von Klitzing who first discovered it in 1980 [Klitzing et al. (1980)]. The fractional quantum Hall effect (where ν is a rational fraction) was discovered only a few years later by Tsui, Störmer, and Gossard [Tsui et al. (1982)].

The single-particle solutions to the Schrödinger equation for this system explain the integer quantum Hall effect. A single electron confined to the $x-y$ plane with a magnetic field in the z-direction is described by the Hamiltonian

$$H = \frac{1}{2\mu}\left(\mathbf{p} + \frac{e}{c}\mathbf{A}(\mathbf{r})\right)^2. \tag{1.1}$$

Choosing the symmetric gauge, $\mathbf{A}(\mathbf{r}) = (1/2)B(-y\hat{x} + x\hat{y})$, the Schrödinger equation, $(H - E)\Psi(\mathbf{r}) = 0$, has eigenenergies

$$E = \frac{1}{2}\hbar\omega_c(2n + 1 + m + |m|) = \frac{1}{2}\hbar\omega_c, \frac{3}{2}\hbar\omega_c, ... \tag{1.2}$$

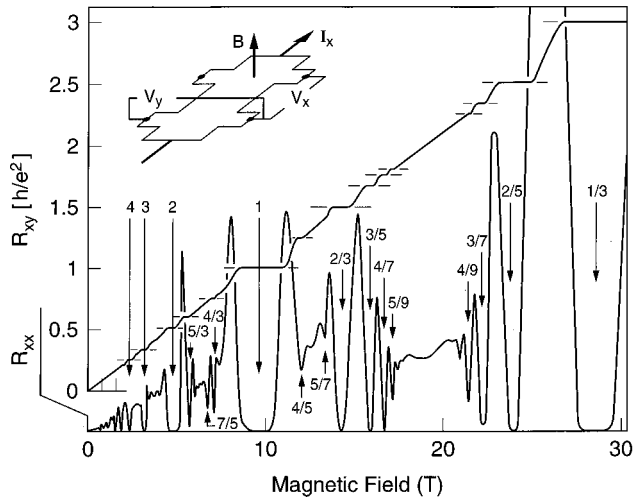

Figure 1.1: $R_{xy} = V_y/I_x$ and the magnetoresistance $R_{xx} = V_x/I_x$. The fractions identify the filling factor, ν. Figure taken from Eisenstein and Stormer (1990).

where ω_c is the cyclotron frequency $eB/\mu c$. Spin is neglected for simplicity as the electron is assumed to be completely spin-polarized by the magnetic field. The energy levels are known as Landau levels [Landau and Lifshitz (1965)] where the lowest Landau level has $n = 0$ and $m = 0, -1, -2, ...$ Although for an infinite sheet the Landau levels are infinitely degenerate, a finite area confines the Landau levels to smaller values of $|m|$, as these are the solutions with the smallest spatial extent. The total number of single-particle states for the lowest Landau level in a finite sample of area A is given by $N_\phi = BA/\phi_0$, where $\phi_0 = hc/e$ is the quantum of magnetic flux. The filling factor ν, then, is N/N_ϕ, the ratio of the total number of particles to the total number of available single-particle states in the lowest Landau level. When ν takes on integer values, the non-interacting system is an incompressible state: any decrease in area or magnetic field will necessarily promote one electron across the energy gap, $\hbar\omega_c$, into the first unoccupied Landau level. The integer quantum Hall effect occurs because the lowest Landau levels are completely filled when ν is an integer, and any increase in ν corresponds to adding electrons to the next energy level.

1.2 The fractional quantum Hall effect

In contrast to the integer quantum Hall effect, the fractional quantum Hall effect cannot be simply described by the single particle solutions and must arise exclusively from electron-electron interactions. For filling factors less than unity, all the electrons lie within the completely degenerate lowest Landau level. Electron-electron interactions alone lift the degeneracy. The quantum Hall system is ideal for studying electron correlations in part because only those interactions lead to the effect. In addition, for exceptionally strong magnetic fields, the electron interaction energies are on a vastly different scale from the single-particle energy levels. Under strong magnetic fields, the Landau level separations are significantly larger than the Coulomb interaction energies, and the electrons can be assumed to all remain in a single Landau level for the simplest problems. The problem of including multiple Landau levels will be addressed in chapter 4.

A significant step in the description of the fractional quantum Hall system came in the form of the Laughlin wavefunction [Laughlin (1983)], an ansatz wavefunction that effectively described the $\nu = 1/(2p+1)$ states, where p is an integer. Using $z = re^{-i\theta}$, the single-particle wavefunction for the lowest Landau level can be written:

$$\psi_{0m}(z) = N_m z^m e^{-|z|^2/4\lambda^2}, \tag{1.3}$$

where N_m is a normalization constant and λ is the magnetic length, $\lambda^2 = \hbar c/eB$. Writing the many-electron wavefunction, $\Psi_\nu(z_1, z_2, ..., z_N)$, for the completely filled lowest Landau level can be done simply with a Slater determinant. The resulting wavefunction is

$$\Psi_1(z_1, z_2, ..., z_N) \propto \prod_{i<j}(z_i - z_j) \times \exp\left(-\frac{1}{4}\sum_k \frac{|z_k|^2}{4\lambda^2}\right). \tag{1.4}$$

Constructing the wavefunction in this manner does not work for the partially filled Landau levels because the single-particle wavefunctions are degenerate. We cannot

simply put the electrons in the lowest-energy single-particle states because all of the available choices have the same energy. However, for the $\nu = 1/(2p+1)$ states, Laughlin proposed the following wavefunction:

$$\Psi_{1/(2p+1)}(z_1, z_2, ..., z_N) \propto \prod_{i<j}(z_i - z_j)^{2p+1} \times \exp\left(-\frac{1}{4}\sum_k \frac{|z_k|^2}{4\lambda^2}\right). \tag{1.5}$$

The Laughlin wavefunction was a remarkable success at describing some of the fractional filling factors. It is antisymmetric under interchange of any electrons (as long as $2p+1$ is odd), reduces the Coulomb repulsion by keeping the electrons farther apart, and describes the correct filling factor, $\nu = 1/(2p+1)$. Curiously, excitations of the Laughlin wavefunction contain quasiparticles, which are collective excitation modes that behave like particles, but carry a charge that is a fraction of the fundamental electron charge, e. The existence of the predicted fractionally charged quasiparticles with charge equal to $e/3$ in excitations of the $\nu = 1/3$ state have been measured experimentally, [Goldman and Su (1995)]. The work of Haldane extended the Laughlin model to predict that quasiparticles of Laughlin states could themselves condense into Laughlin-type states, such as the observed 2/5 and 2/7 states [Haldane (1983)]. However, the Haldane fractional hierarchy model also predicts condensed states at numerous fractional fillings that are not measured experimentally.

A Chern-Simons gauge transformation allows us to consider another description of the system. The Chern-Simons gauge introduces an infinite flux tube with a magnetic flux of $\alpha\phi_0$, where ϕ_0 is again the flux quantum and α is an even integer, onto each electron (or hole) in the system. The resulting Chern-Simons magnetic field is

$$\mathbf{b}(\mathbf{r}) = \alpha\phi_0 \sum_i \delta(\mathbf{r} - \mathbf{r_i})\hat{z}, \tag{1.6}$$

where $\mathbf{r}_i$ is the position of the i-th electron. This magnetic field does not affect the classical motion because the electrons cannot occupy the same location, so no electron experiences the δ-function magnetic field of another electron. However, the

vector potential,

$$\mathbf{a}(\mathbf{r}) = \alpha\phi_0 \int d^2r' \frac{\hat{z} \times (\mathbf{r} - \mathbf{r}')}{|\mathbf{r} - \mathbf{r}'|^2} \Psi^\dagger(r')\Psi(r'), \tag{1.7}$$

does alter the wavefunctions of the particles by introducing a phase factor, as in the Aharonov-Bohm effect. The Hamiltonian including the Chern-Simons gauge is significantly more complicated than the original:

$$H = \frac{1}{2\mu} \int d^2r \Psi^\dagger(r) \left[-i\hbar\nabla_r + \frac{e}{c}\mathbf{A}(\mathbf{r}) + \frac{e}{c}\mathbf{a}(\mathbf{r}) \right]^2 \Psi(r). \tag{1.8}$$

The new Chern-Simons Hamiltonian can be simplified by replacing the electron density operator appearing in Eq.(1.7) with its ground state expectation value,

$$\Psi^\dagger(r')\Psi(r') \;\Rightarrow\; < \Psi^\dagger(r')\Psi(r') >_{gs} = \rho(r') = n_S, \tag{1.9}$$

the average electron density. The mean field Hamiltonian becomes the sum of single-particle Hamiltonians under an effective magnetic field, $B^* = B + \alpha\phi_0 n_S$.

Under this mean field approximation, Jain introduced the composite fermion to explain the observed fractional filling factors [Jain (1989)]. A composite fermion is an electron with an even number, $\alpha = 2p$, of magnetic flux quanta attached. Just as the electron filling factor can be defined by $1/\nu$, the number of flux quanta per electron, the composite fermion filling factor can be defined by $1/\nu^*$ the number of free flux quanta per composite fermion. Then the composite fermion filling factor ν^* is defined by the total number of flux quanta per electron minus the attached flux quanta per electron,

$$\frac{1}{\nu^*} = \frac{1}{\nu} - \alpha. \tag{1.10}$$

When ν^* is an integer, the composite fermions form an incompressible quantum Hall state. When $\nu^* = n$ for n a non-zero integer, then $\nu = n/(\alpha \pm n)$. Choosing $\alpha = 2$ and addition rather than subtraction in the denominator produces the two fractional

quantum Hall sequences, $\nu = 1/3, 2/5, 3/7, ...$ for $n > 0$ and $\nu = 1, 2/3, 3/5, ...$ for $n < 0$, the most prominent fractional quantum Hall states observed.

This mean field Chern-Simons approach is rich and predictive, but the physical interpretation of the Chern-Simons cannot be accurate. In addition to the Coulomb interaction scale, $e^2/\lambda \propto \sqrt{B}$, the Chern-Simons gauge introduces a new energy scale $\hbar\omega_c^* \propto B$. For very large values of the magnetic field, the $\hbar\omega_c^*$ energy should overwhelm the Coulomb energy scale, but the spectra for such systems still resemble the spectra of a fully interacting electron system rather than a non-interacting composite fermion system. It is also the case that neither the Laughlin nor the Jain pictures accommodate a few measured fractional quantum states, notably the $\nu = 5/2$ state. Even though both theoretical descriptions of the fractional quantum Hall system have proven very useful, there remains a great deal of study to be done in the field to understand the behavior of the quantum Hall system. To this end, I will be examining the quantum Hall system using *ab initio* numerical diagonalization studies.

1.3 Numerical studies and pseudopotentials

At this stage, numerical studies are one of the most effective tools used to study the quantum Hall effect. Exact numerical diagonalizations correctly predict the existence of the incompressible quantum liquids at many experimentally measured values of the fractional filling, ν. Numerical diagonalizations are even able to probe the unconventional $\nu = 5/2$ state, which is neither a Laughlin nor a Jain state.

Numerical studies also provide a way to directly study the electronic behavior of the system in a way that experimental measurements currently cannot. Experimental measurements in the quantum Hall system are extremely robust to sample quality, but consist primarily of transport measurements. These measurements are generally of the conductance or resistance tensors, and although the measurements are robust,

stable, and precise, they do not reveal the wavefunctions or the correlative behavior of the electrons in the material.

In contrast to the experimental measurements, numerical studies allow us to more directly examine the exact wavefunctions of the ground state and excited states. For example, the Laughlin ansatz wavefunction correctly predicts the observed experimental behavior of systems with fractional filling given by $\nu = 1/m$, where n is an integer. But it was overlap integrals comparing the trial wavefunction to the results of exact numerical diagonalizations that confirmed the Laughlin wavefunction as the primary contribution to the ground state for $\nu = 1/m$ incompressible states [Laughlin (1983)]. So far, the Laughlin states, $\nu = 1/m$ are the best understood of the condensed states in the fractional quantum Hall system, largely as a result of such numerical studies. The Jain composite fermion picture also offers an explanation of other states in lowest Landau level, and wavefunctions for these condensed states have also been proposed and numerically tested [Dev and Jain (1992)]. For the Jain states again, numerical studies are currently the best method of examining the states.

In addition to the the Laughlin and Jain states, there are also a few unconventional quantum Hall states of great interest, most notably at $\nu = 5/2$. The $\nu = 5/2$ condensed state is the first observed quantum Hall state with an even denominator, and as such clearly does fits into neither the Laughlin nor the Jain picture. A number of possible wavefunctions have been proposed for the 5/2 ground state, but unlike in the Laughlin case, numerical simulations have not yet verified any definitively. It is hoped that the ground state will be dominated by the Moore-Read Pfaffian wavefunction [Moore and Read (1991)], a wavefunction whose quasiparticle excitations would have features that would make them suitable for use as qubits in a functional quantum computer. The actual ground state wavefunction, however, has not yet been determined largely due to challenges in modeling the system numerically, in this case especially due to challenges of incorporating weaker effects into the idealized numerical models.

Numerical techniques have been especially useful in studying the quantum Hall effect, but there are many challenges in exact numerical diagonalizations. One challenge that is somewhat simple to address is the problem of periodic boundary conditions. For the planar system, it is typical to define periodic boundary conditions based on the crystal structure of the system of interest. However, in the quantum Hall system, the periodic structure of the experimental system is largely irrelevant to the observed dynamics of the system, and as a result, there is no preferred origin for the Hamiltonian, (1.1). The problem of periodic boundary conditions is addressed in numerical calculations by using spherical model introduced by Haldane [Haldane (1983)]. The Haldane sphere model maps the quantum Hall plane onto a finite spherical surface. The magnetic field perpendicular to the surface is provided by a magnetic monopole at the sphere's center. Although the surface of the sphere is curved, it is topologically similar to the plane over small regions, and as the sphere's size increases, it better approximates the infinite plane. The model is typically used in numerical diagonalization studies, and it will be the model used in this paper.

Other numerical challenges are not so simple to address as the boundary conditions, however. First, there is a limit to the system size that current computers can handle with exact numerical diagonalization. Typically, the quantum Hall system interaction Hamiltonian for even a single Landau level cannot be calculated for systems with more than only a handful of electrons due to the incredibly large degeneracy of the system. The maximum number of electrons in any for numerical analysis remains less than 20, and is more typically on the order of at most 15. It is challenging to extrapolate the numerical results for small systems to compare them to the experimental results with an Avogadro's number of electrons.

Also problematic are the effects of experimental deviations from the idealized system. Although numerical studies treat the system as though it were an ideal two-dimensional system, the electrons in a quantum Hall system are actually confined only to a very thin layer, and this "finite well width" does affect the electron-electron interactions. Other contributions to the interactions include the chemical

properties of the sample, in-plane magnetic fields, and the concentration of impurities. Another important contribution is that of Landau level mixing. In typical numerical studies, the electrons are treated as being isolated to a single Landau level, but this approximation ignores the fact that the Landau level separation is typically not significantly larger than the Coulomb interaction energy scale. The effect of Landau level mixing has been predicted to be somewhat important for states higher than the lowest Landau level, i.e. states with a filling factor $\nu > 1$.

In the most robust fractional quantum Hall states (e.g. the $\nu = 1/3$ state), these effects are not strong in comparison to the energy gap between the incompressible ground state and the lowest energy excited states. As such, the deviations of the idealized electron system from the actual experimental system are relatively unimportant, and numerical results model the behavior of the stronger states very well. However, the effects of the deviations from the ideal system are more important for some of the more fragile quantum Hall states. Landau level mixing, for example, is believed to be significantly more important in the first excited Landau level than in the lowest. The $\nu = 5/2$ state in particular is believed to be somewhat affected by Landau level mixing [Nayak et al. (2008)], and the effect of Landau level mixing should be incorporated into numerical models in order to better model the system. In addition, the effect of different confinement potentials and other effects may be more important for the less energetically favorable fractional fillings than for the stronger ones.

Some of these factors are extremely challenging to address in numerical models. For example, it is difficult to even know the precise microscopic chemical and structural composition of a given experimental sample, and so including these effects in a numerical model is not feasible. However, it is possible to incorporate some of these effects, such as the finite width effect or Landau level mixing, into numerical models. This can be accomplished by evaluating how these effects modify the pair interactions. The pair interactions and their modifications are the primary focus of

this dissertation. In particular, I will address some of these issues by addressing their effects on the pair interaction function known as the pair pseudopotential.

The pair pseudopotential, developed by Haldane [Prange and Girvin (1987)] and sometimes referred to as the Haldane pseudopotential, is a quantity that expresses the interaction energy of a pair of particles in terms of their total angular momentum. For particles on an infinite plane, the pseudopotential of the n^{th} Landau level is expressed as $V_{n,m}$, where m is the relative z-component of angular momentum of a pair of electrons. In the Haldane sphere model, the pseudopotential $V_n(L)$ of the n^{th} Landau level is given in terms of the pair's total angular momentum L. (The planar azimuthal angular momentum m and the spherical angular momentum L are analogous and easily related, as will be discussed later.) Although the pseudopotential is essentially just a simple one-to-one function of the angular momentum, it actually contains all of the information of the electron dynamics of the system. For instance, the energy spectrum and dynamics of a system of N particles in the n^{th} Landau level can be calculated entirely from the set of pair energies given by $V_{n,m}$ or $V_n(L)$. Even more remarkably, the distinction between the different Landau levels is entirely contained within the pseudopotential: the pseudopotential indices are the only independent parameters that determine the electronic spectrum in strong magnetic fields. (That the problem in any Landau level can be mapped into the lowest Landau level can be most easily seen by using raising and lowering operators in the planar system [Simon et al. (2007)]).

The pseudopotential has proven to be a valuable tool for understanding the behavior of the quantum Hall system. The Laughlin $\nu = 1/m$ states in LL0, where m is an odd integer, are well understood in terms of the pair pseudopotential. Laughlin correlations, which characterize the Laughlin states, occur when electron pairs avoid states with the highest allowed angular momentum, L [Prange and Girvin (1987)]. It is the pseudopotential behavior which drives these correlations. For example, it can be rigorously shown that a harmonic pseudopotential, a pseudopotential of the form $V(L) = a + bL(L+1)$ does not break the degeneracy of n-particle angular momentum

multiplets and does not introduce correlations into the quantum Hall system [Wójs and Quinn (1998); Quinn and Wójs (2000)]. Correlations are induced in the system by deviations from a harmonic pseudopotential: Laughlin correlations in particular arise when the pseudopotential increases more rapidly than the harmonic pseudopotential for the highest allowed pair angular momentum values (a pseudopotential of this type is called "superharmonic"). Electron pairs under the influence of a superharmonic pseudopotential lower their energy by avoiding the highest angular momentum pair states: in other words, they will be Laughlin correlated.

The pseudopotential description for correlations in the system also offers an explanation for why only some possible daughter states of the Jain states have been observed. Under the mean field description of Jain, incompressible quantum liquid states form at electron filling factors which correspond to a completely filled integral number of non-interacting quasiparticle Landau levels. Such states occur at electron fillings of $\nu = n(\alpha n \pm 1)^{-1}$, where α is an even integer. For a partially filled composite fermion Landau level, the interactions between the composite fermions could give rise to incompressible daughter states, but only some of those have been observed [Pan et al. (2003)]. It has been shown by the group at the University of Tennessee that composite fermions of the Jain picture are not non-interacting fermions, and that their interaction energies, the quasiparticle pseudopotentials, determine the formation of the daughter states [Sitko et al. (1996); Yi and Quinn (1997)]. These quasiparticle pseudopotentials can currently only be studied through numerical diagonalization, and are themselves dependent wholly on the electron pseudopotential of the system.

The numerical evaluations of the electron and quasiparticle pseudopotentials have proven effective at explaining many of the observed states in the lowest Landau level, LL0. However, in the electron LL1 as well as in the composite fermion LL1, the situation is rather more complicated. Many of the most robust incompressible quantum liquid states observed in LL0 have not been observed in LL1, and visa-versa. In LL0, the most robust of the observed quantum Hall states are the $\nu = 1/3$ and $2/3$ states, followed by $\nu = 2/5$ and $3/5$, and $\nu = 3/7$ and $4/7$. It is reasonable to

expect similar condensed states in LL1 at $\nu = 2 + \nu_0$, where ν_0 is an observed LL0 fractional filling. (States in LL1 are written as $\nu = 2 + q/p$, where q/p is a fraction between 0 and 1, to indicate that both LL0 spin levels are totally filled.) However, the corresponding fractional fillings in LL1, $\nu = 2+2/5, 2+3/5, 2+3/7$ and $2+4/7$, have not been observed experimentally [Pan et al. (2003)]. In addition, the first excited Landau level also has a robust condensed state at $\nu = 2 + 1/2$, for which there is no observed counterpart at $\nu = 1/2$ in LL0.

The observed differences between LL0 and LL1 arise entirely from the differences, possibly even from small differences, in their electron pseudopotentials. In addition, the quasiparticle pseudopotentials should also be sensitive to changes in the electron pseudopotentials. While the unaltered Coulomb pseudopotential seems to give accurate enough results to effectively model the quantum Hall system in the lowest Landau level, the effect of finite-well widths and Landau level mixing may be more significant in the first excited Landau level. Because the pseudopotential is the key dynamic parameter for the quantum Hall effect, in this dissertation, I will derive novel analytic expressions for the pseudopotential on the Haldane sphere and will address how Landau level mixing affects the pseudopotentials.

1.4 Outline of this dissertation

In Chapter 2, I will first review the single-particle solutions and the Haldane sphere model. I will derive analytic expressions for the two-body matrix elements and the pair pseudopotentials on the Haldane sphere using the well-understood framework of angular momentum algebra. The new analytic expressions will extend the results of [G. Fano (1986)] to any Landau level and will allow the direct calculation of interactions between particles in different Landau levels. After comparing my expressions to the pseudopotentials calculated on an infinite plane, I will describe how finite well effects can be incorporated into the pair pseudopotential in this model. Finally, I will derive a way to invert the pair pseudopotential to recover the actual

interaction potential, $V(r_{ij})$. This technique can provide extra insight into proposed model pseudopotentials and may be helpful in suggesting ways to engineer samples to produce desired quantum states.

Chapter 3 will consist primarily of explaining how to extend the two-particle matrix elements and pair pseudopotentials to a system of n electrons in a single Landau level. Calculations in the n-body system will require the use of Slater determinants to perform configuration interaction calculations. I will discuss the selection of the restricted Hilbert space of the problem and the application of the Wigner-Eckart theorem to the problem. I will then present some straight forward numerical results and discuss them in the framework of the composite fermion picture and the Laughlin hierarchy of fractional fillings. Finally, I will derive expressions for calculating the relative prevalence of angular momentum pair states and the coefficients of fractional grandparentage using the Slater determinant framework.

Finally, in Chapter 4, I will use the results of Chapter 2 and a modification of the methods explained in Chapter 3 in order to calculate the effect of Landau level mixing on the pair pseudopotentials. I will first cover the simpler case of the lowest Landau level, and then move into the more complex calculations for the first excited Landau level. Finally, I will discuss my results in the context of other works that have addressed Landau level mixing using other techniques, such as perturbation theory.

Chapter 2

Analytic Solutions

2.1 Solutions on the plane and background

In order to examine the many-body dynamics of the quantum Hall system, it is useful to first describe the behavior of a single electron in the system. For a single electron confined to an infinitely thin two-dimensional metallic plane in the presence of a magnetic field normal to the plane, $\mathbf{B} = B\hat{z}$, the Hamiltonian is

$$H = \frac{1}{2\mu}\left(\mathbf{p} + \frac{e}{c}\mathbf{A}\right). \tag{2.1}$$

In the symmetric gauge, $\mathbf{A}(\mathbf{r}) = \frac{1}{2}\mathbf{r} \times \mathbf{B}$, the Schrödinger equation $(H - E)\Psi(\mathbf{r}) = 0$ has eigenstates

$$\Psi_{n,m}(r, \phi) = \mathcal{N}_{n,m} e^{im\phi} \xi^{|m|} e^{-\xi^2/4} L_n^{|m|}(\xi^2/2) \tag{2.2}$$

where $\xi = r/\lambda_0$ is the radius scaled by the magnetic length, $\lambda_0 = \sqrt{eB/\hbar c}$, and the functions $L_n^{|m|}$ are the associated Laguerre polynomials. The indices n and m are the principle and angular quantum numbers, respectively. Both are integers, n is always non-negative, and m is unbounded. The normalization constant $\mathcal{N}_{n,m}$ is given by

$$\mathcal{N}_{n,m} = (-1)^n \left[\frac{n!}{2\pi(|m| + n)! 2^{|m|}}\right]^{1/2}. \tag{2.3}$$

The eigenstates have energies given by

$$E_{n,m} = \frac{1}{2}\hbar\omega_c \left(2n + 1 + m + |m|\right), \tag{2.4}$$

where $\omega_c = eB/\mu_e c$ is the cyclotron frequency of an electron with effectivce mass μ_e. The energies are evenly separated by integral multiples of $\hbar\omega_c$ as in the case of the harmonic oscillator, and are called Landau levels. But unlike the energy levels of the harmonic oscillator, the Landau levels are highly degenerate for $m < 0$. On an infinite sheet, the degeneracy is also infinite, but on a finite sheet of area πR^2, the degeneracy of the lowest Landau level is $N_\phi = \pi R^2 B/\phi_0$, where $\phi_0 = h/e$ is the fundamental quantum of magnetic flux.

The non-interacting electron picture explains the integer quantum Hall effect. If N non-interacting electrons are added to the surface at very cold temperatures, the electrons will fall into the lowest available Landau levels. At integral values of the filling factor, $\nu = N/N_\phi$, the addition of a single electron (or any infinitesimal reduction of the area or magnetic field) must overcome an energy gap of $\hbar\omega_c$. Because reducing the area of the sample requires promotion of electrons across an energy gap, the system is called incompressible. These incompressible quantum liquid states are dramatically visible in transport measurements at low temperatures, as seen at integer values of ν in figure 1.1. In particular, the longitudinal resistance of the sample characteristically drops dramatically at integral values of the filling factor, and the Hall resistance plateaus at values of $\nu h/e^2$.

The non-interacting electron picture explains the presence of incompressible states at integer filling factors. However, the incompressible states at non-integer fillings arise entirely due to correlated electron behavior. In order to better analyze the incompressible states of these highly correlated systems, it is particularly convenient to avoid the edge effects of the quantum Hall disk by instead carrying out numerical diagonalizations in a model system known as the Haldane sphere.

2.2 Monopole harmonics and the Haldane sphere

The Haldane sphere model maps the infinitely thin, two-dimensional metallic surface of the quantum Hall system onto the surface of a sphere in order to eliminate boundary conditions and to take advantage of the rotational and translational symmetry of the physical problem. The mapping is conformal: it preserves angles, but not areas. (The inverse mapping, from the sphere onto the plane, is known as a stereographic projection.) As in the planar model of the quantum Hall effect, the magnetic field must be uniform and perpendicular to the surface at all points. The magnetic field is provided by a Dirac magnetic monopole at the center of the sphere of strength $2Q\phi_0$, where the quantity $2Q$ is an integer, and $\phi_0 = h/e$ is, again, the fundamental quantum of magnetic flux. The resulting magnetic field at the surface of the sphere with radius R_s is directed radially outward:

$$\mathbf{B} = \frac{2Q\phi_0}{4\pi R_s^2}\hat{R}. \tag{2.5}$$

In the spherical system, the single particle Hamiltonian,

$$\hat{H}_0 = \frac{1}{2mR_s^2}\left(\hat{\mathbf{L}}^2 - \hbar^2 Q^2\right), \tag{2.6}$$

is a function of the standard angular momentum operator, $\hat{\mathbf{L}}$. The single particle solutions of the Schrödinger equation are known as the monopole harmonics, written $Y_{Q,l,m}$ or $|Q,l,m\rangle$. The quantum numbers l and m are the standard shell angular momentum and azimuthal quantum numbers, respectively, and Q is the magnetic monopole strength. The monopole harmonics satisfy the usual angular momentum eigenvalue equations,

$$\mathbf{l}^2|Q,l,m\rangle = \hbar^2 l(l+1)|Q,l,m\rangle \tag{2.7}$$

$$\mathbf{l_z}|Q,l,m\rangle = \hbar m|Q,l,m\rangle. \tag{2.8}$$

In the case of $Q = 0$, the monopole harmonics are exactly the well-known spherical harmonics.

The eigenenergies of the single-particle Hamiltonian are independent of the azimuthal quantum number, m:

$$\mathcal{E}_{Q,l,m} = \frac{\hbar\omega_c}{2Q}\left[l(l+1) - Q^2\right]. \tag{2.9}$$

Because the energy must be positive, the allowed values of l are given by $l_n = Q + n$ where $n = 0, 1, 2, etc\ldots$ is the Landau level index, and the energy is approximately equal to $E_n \approx \hbar\omega_c\,(n + 1/2)$ for large Q. As in the case of the spherical harmonics, the azimuthal quantum number m is constrained by the shell angular momentum, $-l \leq m \leq l$. The energy in the n^{th} Landau level, being independent of m, is clearly $(2l_n + 1)$-fold degenerate.

The complete single-particle Hilbert space is the infinite set of all monopole harmonics sharing the same magnetic quantum number Q, since l_i has no upper bound. Fortunately, for typical quantum Hall problems, it is reasonable to restrict the acting Hilbert space significantly. For example, it is typical to restrict the Hilbert space to a single isolated Landau level because, for sufficiently strong magnetic fields, the Landau level separation $\hbar\omega_c$ is much larger than the typical Coulomb electron-electron energy. As a result of the large inter-Landau level spacing, individual Landau levels can be considered essentially isolated, and it is a good approximation to ignore the possibility of electron excitations between Landau levels in such cases.

2.3 Two-body matrix elements on the Haldane sphere

I will begin with the expression for a general matrix element of a two-body scalar operator $\hat{V}$. A general matrix element can be written as $\langle Q, l_1', m_1'; Q, l_2', m_2'|\hat{V}|Q, l_1, m_1; Q, l_2, m_2\rangle$.

The matrix element expression is equal to the integral over the two particle coordinates $\mathbf{r}_1$ and $\mathbf{r}_2$ of the initial and final occupied monopole harmonic wavefunctions:

$$\langle Q, l_1', m_1'; l_2', m_2' | \hat{V} | Q, l_1, m_1; l_2, m_2 \rangle = \int Y^*_{Q,l_1,m_1'}(\mathbf{r}_1) Y^*_{Q,l_2',m_2'}(\mathbf{r}_2) \hat{V}(\mathbf{r}_1, \mathbf{r}_2) Y_{Q,l_1,m_1}(\mathbf{r}_1) Y_{Q,l_2,m_2}(\mathbf{r}_2) d^3\mathbf{r}_1 d^3\mathbf{r}_2. \tag{2.10}$$

In the Haldane sphere system, the monopole strength is the same for all particles, so $Q_1 = Q_2$, and we have dropped the label on Q. Note that, in the pair matrix element expressions, the state vector $|Q, l_1, m_1; l_2, m_2\rangle$ is not explicitly antisymmetrized.

If the potential V is a function of $|\mathbf{r}_1 - \mathbf{r_2}|$ (as is the case for the Coulomb potential), it can expanded in Legendre polynomials,

$$V(|\mathbf{r}_1 - \mathbf{r_2}|) = \frac{e^2}{4\pi\epsilon} \sum_{k=0}^{\infty} (2k+1) V_k(r_1, r_2) P_k(\cos\theta_{12}), \tag{2.11}$$

where

$$V_k(r_1, r_2) = \frac{1}{2} \int_0^{\pi} V(r_{12}) P_k(\cos\theta) \sin\theta d\theta. \tag{2.12}$$

The angle between the two particles in (2.11) is θ_{12}, and ϵ is the dielectric constant of the material.

For a spherical shell of radius R_s, the electrons both lie at the same radius $r_< = r_> = R_s$, and (2.11) can be rewritten in terms of a new set of parameters, V_k. The V_k are unitless coefficients that define the potential; for the Coulomb potential, $V_k = 1$ for all values of k. Other choices of V_k representing other potentials and are also possible. For an infinitely thin spherical shell, the potential is a Dirac delta function in the radial direction for both particles, and so the potential becomes, when combining (2.10) and (2.11)

$$V(|\mathbf{r}_1 - \mathbf{r_2}|) = \frac{e^2}{4\pi\epsilon R_s} \sum_{k=0}^{\infty} V_k P_k(\cos\theta_{12}) \delta(|r_1| - R_s) \delta(|r_2| - R_s), \tag{2.13}$$

where $\delta(|r_i| - R_s)$ is a Dirac delta function in the radius of the i^{th} particle. The radius of the sphere, $R_s = \lambda_0\sqrt{Q}$ is given in terms of the magnetic length, $\lambda_0 = \sqrt{\hbar/(eB)}$. Substituting (2.13) into (2.10) and integrating over the radial coordinates yields the matrix elements as an integral over only the angular coordinates of the two particles,

$$\langle Q, l_1', m_1'; l_2', m_2' | V | Q, l_1, m_1; l_2, m_2 \rangle =$$
$$\left(\frac{e^2}{4\pi\epsilon\lambda_0}\right)\frac{1}{\sqrt{Q}}\int Y^*_{Q,l_1,m_1'}(\mathbf{r}_1)Y^*_{Q,l_2',m_2'}(\mathbf{r}_2)\sum_{k=0}^{\infty}V_k P_k(\cos\theta_{12})Y_{Q,l_1,m_1}(\mathbf{r}_1)Y_{Q,l_2,m_2}(\mathbf{r}_2)d\Omega_1 d\Omega_2, \tag{2.14}$$

where Ω_i represents the angular coordinates, θ_i and ϕ_i of the i^{th} particle.

The evaluation of the matrix element in (2.14) would simplify significantly if we could separate the two coordinate integral into the product of two independent integrals over the particles. Fortunately, according to the well known spherical harmonics addition theorem, the Legendre polynomials separate exactly as hoped,

$$P_k(\cos\theta_{12}) = \frac{4\pi}{2k+1}\sum_{m=-k}^{k} Y^*_{k,m}(\Omega_1)Y_{k,m}(\Omega_2). \tag{2.15}$$

Combining (2.15) and (2.14) yields a separable integral for the matrix elements, given in units of the Coulomb energy $e^2/4\pi\epsilon\lambda_0$:

$$\langle Q, l_1', m_1'; l_2', m_2' | \hat{V} | Q, l_1, m_1; l_2, m_2 \rangle =$$
$$\frac{1}{\sqrt{Q}}\sum_{k=0}^{\infty}\sum_{m=-k}^{k}\frac{4\pi}{2k+1}V_k\int Y^*_{Q,l_1',m_1'}(\Omega_1)Y^*_{k,m}(\Omega_1)Y_{Q,l_1,m_1}(\Omega_1)d\Omega_1$$
$$\times\int Y^*_{Q,l_2',m_2'}(\Omega_2)Y_{k,m}(\Omega_2)Y_{Q,l_2,m_2}(\Omega_2)d\Omega_2 \tag{2.16}$$

The two integrals can be evaluated by using the results of Wu and Yang, [Wu and Yang (1976)] and [Wu and Yang (1977)]. First, we explicitly substitute the monopole

harmonic with $Q = 0$ for the spherical harmonics in (2.16),

$$Y_{l,m} = Y_{0,l,m}. \tag{2.17}$$

We then use *Theorem 1* from [Wu and Yang (1977)],

$$Y^*_{Q,l,m} = (-1)^{Q+m} Y_{-Q,l,-m}, \tag{2.18}$$

to rewrite (2.16) so that we can use *Theorem 3* from [Wu and Yang (1977)], which states *if* $Q + Q' + Q'' = 0$ *and* $m + m' + m'' = 0$, *then*

$$\int Y_{Q,l,m} Y_{Q',l',m'} Y_{Q'',l'',m''} d\Omega = (-1)^{l+l'+l''} \left[\frac{(2l+1)(2l'+1)(2l''+1)}{4\pi}\right]^{1/2} \begin{pmatrix} l & l' & l'' \\ m & m' & m'' \end{pmatrix} \begin{pmatrix} l & l' & l'' \\ Q & Q' & Q'' \end{pmatrix} \tag{2.19}$$

where the round brackets are 3j symbols. Although *Theorem 3* explicitly states that $m + m' + m'' = 0$ is a necessary condition for the evaluation of the theorem, their subsequent proof actually does not rely on the assumption, although it does require $q + q' + q'' = 0$. It is the case that integral is non-zero only when $m + m' + m'' = 0$, but this is a consequence of monopole harmonics' relation to the standard rotation functions. In one region of the sphere, for example, Wu and Yang define the monopole harmonics in terms of the rotation functions of [Edmonds (1996)].

$$Y_{Q,l,m} = \left[\frac{2l+1}{4\pi}\right] e^{i(q+m)\phi} d^{(l)}_{-m,q}\theta. \tag{2.20}$$

The integral over the ϕ variable in 2.19 gives 0 unless $m + m' + m'' + q + q' + q'' = 0$. Since $q + q' + q'' = 0$ is required, it follows that the integral is non-zero except when the sum over the m's is also zero. This information is also contained in the 3j symbols, which are zero under the same circumstances.

Combining the theorems of Wu and Yang, with (2.16)

$$\langle Q, l_1', m_1'; l_2', m_2' | \hat{V} | Q, l_1, m_1; l_2, m_2 \rangle =$$
$$\frac{1}{\sqrt{Q}} \sum_{k=0}^{\infty} \sum_{m=-k}^{k} V_k (-1)^{2Q+m2'+m_1+l_1'+l_2'+l_1+l_2} \left[(2l_1'+1)(2l_2'+1)(2l_1+1)(2l_2+1) \right]^{1/2}$$
$$\times \begin{pmatrix} l_1' & k & l_1 \\ -m_1' & -m & m_1 \end{pmatrix} \begin{pmatrix} l_1' & k & l_1 \\ -Q & 0 & Q \end{pmatrix} \begin{pmatrix} l_2' & k & l_2 \\ -m_2' & m & m_2 \end{pmatrix} \begin{pmatrix} l_2' & k & l_2 \\ -Q & 0 & Q \end{pmatrix}. \tag{2.21}$$

The sums over m and k simplify using the properties of the 3j symbols [Edmonds (1996)]. Any general 3j symbol,

$$\begin{pmatrix} j_1 & j_2 & j_3 \\ m_1 & m_2 & m_3 \end{pmatrix}, \tag{2.22}$$

is non-zero only when $m_1 + m_2 + m_3 = 0$ and when j_1, j_2, and j_3 together satisfy the triangle inequality, $|j_1 - j_2| \leq j_3 \leq j_1 + j_2$. As such, the sum over m collapses, and $m = m_1 - m_1' = m_2' - m_2$. The triangle inequality requirement means that the sum over infinite values of k is actually a finite sum up to k_{max}, which is the largest value of k which satisfies the triangle condition for both the sets $\{l_1', k, l_1\}$ and $\{l_2', k, l_2\}$.

And so, applying all these reductions to (2.21), we get the final expression for a two-particle matrix element on the Haldane sphere:

$$\langle Q, l_1', m_1'; l_2', m_2' | \hat{V} | Q, l_1, m_1; l_2, m_2 \rangle =$$
$$\frac{1}{\sqrt{Q}} \sum_{k=0}^{k_{max}} V_k (-1)^{2Q+m2'+m_1+l_1'+l_2'+l_1+l_2} \left[(2l_1'+1)(2l_2'+1)(2l_1+1)(2l_2+1) \right]^{1/2}$$
$$\begin{pmatrix} l_1' & k & l_1 \\ -m_1' & m_1 - m_1' & m_1 \end{pmatrix} \begin{pmatrix} l_1' & k & l_1 \\ -Q & 0 & Q \end{pmatrix} \begin{pmatrix} l_2' & k & l_2 \\ -m_2' & m_2' - m_2 & m_2 \end{pmatrix} \begin{pmatrix} l_2' & k & l_2 \\ -Q & 0 & Q \end{pmatrix}. \tag{2.23}$$

The matrix element is given in units of the Coulomb energy, $e^2/4\pi\epsilon\lambda_0$, where $\lambda_0 = \sqrt{\hbar/eB}$ is, again, the magnetic length.

2.4 Pair pseudopotentials

The pair pseudopotential $V(L_2)$ is defined as the interaction energy of a pair of electrons as a function of their pair angular momentum. Although the pseudopotential is a function only of the pair angular momentum, $V(L_2)$ actually contains all of the correlative behaviors of any n-body system, and can be used in the place of the two-body matrix elements calculated above to perform the same calculations. The pseudopotential is defined on the Haldane sphere by using standard angular momentum coupling to expand the monopole harmonics into a coupled basis,

$$|Q, l_1, m_1; l_2, m_2\rangle = \sum_{L,M} |Q, l_1, l_2; L, M\rangle\langle Q, l_1, l_2; L, M|Q, l_1, m_1; l_2, m_2\rangle. \tag{2.24}$$

Equation (2.24) is analogous to equation (3.5.2) in [Edmonds (1996)], except that the angular momentum eigenvectors, $|Q, l_1, l_2; LM\rangle$, are comprised of the monopole harmonics. The expression $\langle Q, l_1, l_2; L, M|Q, l_1, m_1; l_2, m_2\rangle$ is an ordinary Clebsch-Gordan coefficient [Wu and Yang (1976)]. Note here that the angular momentum eigenvectors $|Q, l_1, l_2; LM\rangle$ are neither explicitly symmetrized nor antisymmetrized; as in the previous section, particle exchange and wavefunction symmetry have not been included in this derivation. The symmetry of the angular momentum eigenstates will instead be addressed in the following section.

And so, if we expand both the initial and final state vectors in the coupled angular momentum basis, we can rewrite the two-body matrix element in the following form:

$$\langle Q, l_1', m_1'; l_2', m_2' | V(|r_{12}|) | Q, l_1, m_1; l_2, m_2 \rangle = \sum_{L',M'} \sum_{L,M} \langle Q, l_1', m_1'; l_2', m_2' | Q, l_1', l_2'; L', M' \rangle \times \langle Q, l_1', l_2'; L', M' | V(|r_{12}|) | Q, l_1, l_2; L, M \rangle \langle Q, l_1, l_2; L, M | Q, l_1, m_1; l_2, m_2 \rangle. \tag{2.25}$$

In this expression, the pseudopotential, $V(L)$ for particles in a single Landau level is evaluated from the matrix element from (2.25),

$$\langle Q, l_1', l_2'; L', M' | V(|r_{12}|) | Q, l_1, l_2; L, M \rangle. \tag{2.26}$$

For particles in the n^{th} Landau level, that is, when $l = Q + n = l_1 = l_2 = l_1' = l_2'$, this matrix element gives the pair pseudopotential.

As before, we write the scalar potential, $V(r_{12})$, in units of the Coulomb energy as the sum over Legendre polynomials,

$$V(\hat{r}_1, \hat{r}_2) = \frac{1}{\sqrt{Q}} \sum_k V_k P_k(\cos\theta_{12}). \tag{2.27}$$

In order to acquire the pseudopotential, I will use tensor operators, and so it is useful here to use Racah notation to express the potential. From [Edmonds (1996)] Eq. (2.5.31), the spherical harmonics in Racah notation are

$$C_q^{(k)} = \left(\frac{4\pi}{2k+1} \right)^{1/2} Y_{kq}(\theta, \phi). \tag{2.28}$$

In this notation, the spherical harmonic addition theorem (2.15) is

$$P_k(\cos\theta_{12}) = \sum_q C_q^{(k)*}(\theta_1, \phi_1) C_q^{(k)}(\theta_2, \phi_2). \tag{2.29}$$

The Legendre polynomial $P_k(\cos\theta)$ can also be considered a scalar product of two $\mathbf{C}^{(k)}$ tensors of different arguments:

$$P_k(\cos\theta_{12}) = \left[\mathbf{C}^{(k)}(\theta_1,\phi_1)\cdot\mathbf{C}^{(k)}(\theta_2,\phi_2)\right]^0_0 \tag{2.30}$$

where the final superscript and subscript indicate that the enclosed product is scalar, a tensor of rank 0.

Using [Edmonds (1996)] equation (7.1.6), the evaluation of a matrix element of the scalar product of two tensors of rank k is given by the following equation:

$$\langle Q,l_1',l_2';L',M'|\left[\mathbf{C}^{(k)}(\theta_1,\phi_1)\cdot\mathbf{C}^{(k)}(\theta_2,\phi_2)\right]^0_0|Q,l_1,l_2;L,M\rangle = (-1)^{l_1+l_2'+L}\delta_{L,L'}\delta_{M,M'}\begin{Bmatrix} L & l_2' & l_1' \\ k & l_1 & l_2 \end{Bmatrix}\sum_\gamma (Q,l_1'||\mathbf{C}^{(k)}(\hat{r}_1)||\gamma,l_1)(\gamma,l_2'||\mathbf{C}^{(k)}(\hat{r}_2)||Q,l_2). \tag{2.31}$$

The expression $(Q,l_1'||\mathbf{C}^{(k)}(\hat{r}_1)||\gamma,l_1)$ is known as a reduced matrix element. The reduced matrix elements are evaluated using [Edmonds (1996)] equation (5.4.1), which is a statement of the Wigner-Eckart theorem:

$$\langle Q,l',m'|C_x^{(k)}|\gamma,l,m\rangle = (-1)^{l'-m'}\begin{pmatrix} l' & k & l \\ -m' & x & m \end{pmatrix}(Q,l'||\mathbf{C}^{(k)}||\gamma,l). \tag{2.32}$$

The expression on the left of (2.32) is also given by

$$\langle Q,l',m'|C_x^{(k)}|\gamma,l,m\rangle = \left(\frac{4\pi}{(2k+1)}\right)^{1/2}\int Y^*_{Q,l',m'}Y_{0,k,x}Y_{\gamma,l,m}d\Omega, \tag{2.33}$$

which can also be evaluated using the equation (1) of [Wu and Yang (1977)] to yield

$$\langle Q,l',m'|C_x^{(k)}|\gamma,l,m\rangle = (-1)^{Q+m'+l'+l+k}\left[(2l'+1)(2l+1)\right]^{1/2}\begin{pmatrix} l' & k & l \\ -m' & x & m \end{pmatrix}\begin{pmatrix} l' & k & l \\ -Q & 0 & \gamma \end{pmatrix} \tag{2.34}$$

By combining (2.32) and (2.34),we get an expression for the reduced matrix element

$$(Q,l'||\mathbf{C}^{(k)}||\gamma,l) = (-1)^{Q+2m'+l+k}\left[(2l'+1)(2l+1)\right]^{1/2}\begin{pmatrix} l' & k & l \\ -Q & 0 & \gamma \end{pmatrix}. \tag{2.35}$$

Note that, because of the symmetry properties of the 3j symbol in (2.35), the reduced matrix element is non-zero only when $\gamma = Q$, which collapses the sum in (2.31).

In order to reduce the following expression slightly, we note that k is an integer. In addition, because m' and m'' are always both integers or both odd-half integers, then $m' + m''$ is also always an integer. As a result, we have already included $(-1)^{2k+2(m'+m'')} = 1$ in the expression for simplicity. Substituting (2.34) into (2.30) gives the expression for a two-body matrix element independent of azimuthal quantum numbers, m_i:

$$\begin{aligned}\langle Q,l_1',l_2';L',M'|V(|r_{12}|)|Q,l_1,l_2;L,M\rangle = \\ \frac{1}{\sqrt{Q}}\sum_{k=0}^{k_{max}} V_k(-1)^{2Q+L+2l_1+l_2+l_2'}\left[(2l_1'+1)(2l_1+1)(2l_2'+1)(2l_2+1)\right]^{1/2} \\ \times\begin{Bmatrix} L & l_2' & l_1' \\ k & l_1 & l_2 \end{Bmatrix}\begin{pmatrix} l_1' & k & l_1 \\ -Q & 0 & Q \end{pmatrix}\begin{pmatrix} l_2' & k & l_2 \\ -Q & 0 & Q \end{pmatrix}\end{aligned} \tag{2.36}$$

The pair pseudopotential is defined as the expectation value of the potential for a pair of particles in Landau level n, abbreviated LLn, as a function of their total angular momentum, L. On the Haldane sphere, the n^{th} Landau level is the angular momentum shell defined by $l = Q + n$, and the n^{th} Landau level pseudopotential $V_{l,Q}(L) = (\langle Q,l,l;L,M|V(|r_{12}|)|Q,l,l;L,M\rangle$ in Coulomb units is

given by the following expression:

$$V_{l,Q}(L) = \frac{1}{\sqrt{Q}} \sum_{k=0}^{2l} V_k (-1)^{2Q+L} (2l+1)^2 \begin{Bmatrix} L & l & l \\ k & l & l \end{Bmatrix} \begin{pmatrix} l & k & l \\ -Q & 0 & Q \end{pmatrix}^2 \tag{2.37}$$

where $l = Q + n$ is the shell angular momentum of the n^{th} Landau level.

2.5 Symmetry of angular momentum eigenstates

Before comparing equation (2.37) to previously published results for the pseudopotentials, this section will briefly cover the particle exchange and symmetry for the coupled angular momentum states. In the previous section, the angular momentum eigenstates, denoted $|Q, l, l'; L, M\rangle$, are not explicitly symmetric or antisymmetric. In order to construct an antisymmetric wavefunction from the eigenstates of the total angular momentum, we begin again with the results of Wu and Yang.

The wavefunction for a pair of particles in the field of a magnetic monopole is a coupled monopole harmonic state, $F_{Q,Q',L,M}(\mathbf{r}_1, \mathbf{r}_2)$ according to *Appendix D* from [Wu and Yang (1976)]. This wavefunction is the projection into coordinate space of the ket $|Q, l, l'; L, M\rangle$. The two-body wavefunction, $F_{Q,Q',L,M}$, transforms under the simultaneous rotation of θ and ϕ in the same manner as the ordinary spherical harmonics, the $Y_{l,m}$, and obeys the following equation:

$$F_{Q,Q',L,M}(\mathbf{r}_1, \mathbf{r}_2) = \sum_{m,m'} Y_{Q,l,m}(\mathbf{r}_1) Y_{Q',l',m'}(\mathbf{r}_2) \langle ll'LM|lml'm'\rangle. \tag{2.38}$$

The Clebsch-Gordan coefficients, $\langle ll'LM|lml'm'\rangle$, are as defined in [Edmonds (1996)]. After such a rotation, the problem will be set in a different gauge. However, the different gauge does not affect the particle exchange discussion here.

Particle exchange can be addressed by directly applying the two-particle permutation operator, $P_{1,2}$, which exchanges particles 1 and 2, to (2.38).

$$P_{1,2}F_{Q,Q',L,M}(\mathbf{r}_1,\mathbf{r}_2) = \sum_{m,m'} Y_{Q,l,m}(\mathbf{r}_2)Y_{Q',l',m'}(\mathbf{r}_1)\langle ll'LM|lml'm'\rangle\langle ll'LM|lml'm'\rangle \tag{2.39}$$

Since the Clebsch-Gordan coefficients obey the following symmetry property, given in [Edmonds (1996)] equation (3.5.14):

$$(j_a m_a j_b m_b|j_a j_b jm) = (-1)^{j_a+j_b-j}(j_b m_b j_a m_a|j_b j_a jm), \tag{2.40}$$

we can rewrite (2.39) as

$$P_{1,2}F_{Q,Q',L,M}(\mathbf{r}_1,\mathbf{r}_2) = (-1)^{l+l'-L}\sum_{m,m'} Y_{Q,l,m}(\mathbf{r}_2)Y_{Q',l',m'}(\mathbf{r}_1)\langle l'\ lLM|l'm'\ lm\rangle. \tag{2.41}$$

Simplifying (2.41) and rewriting in ket notation gives the simple expression

$$P_{1,2}|Q,l\ l'LM\rangle = (-1)^{l+l'-L}|Q,l'\ lLM\rangle. \tag{2.42}$$

As a result, we can symmetrize an angular momentum eigenstate with the unnormalized two-particle symmetrization operator,

$$\hat{S}_2 = (1 + P_{1,2})\,. \tag{2.43}$$

Likewise, we can antisymmetrize an angular momentum eigenstate with the unnormalized two-particle antisymmetrization operator,

$$\hat{A}_2 = (1 - P_{1,2})\,. \tag{2.44}$$

For electron pairs in the Haldane sphere system, both the symmetric and antisymmetric spatial pair states apply because both spin states, up and down,

are allowed for either particle. According to the Pauli exclusion principle, the wavefunction for fermions must be fully antisymmetric under particle exchange, but the full wavefunction includes the spatial wavefunctions and the spin functions. Although the spin and spatial wavefunctions are not separable for many-body systems, they are separable in the case of two-body systems. As such, a pair of electrons with a symmetric spin wavefunction (i.e. in a triplet state spin configuration) must have an antisymmetric spatial wavefunction. Likewise, the spatial wavefunction of a pair of electrons in singlet spin state must be symmetric.

In a typical quantum Hall experiment, the magnetic field of the system is strong enough that it is reasonable to assume that the electrons will be totally spin polarized. Because spin aligned electron pairs must be in a spin triplet state, the spatial wavefunction is guaranteed to be antisymmetric. Their angular momentum eigenstate on the Haldane sphere must then be

$$|Q,l,l';L,M\rangle_A = \frac{1}{\sqrt{2}}\left[|Q,l,l';L,M\rangle - (-1)^{l+l'-L}|Q,l',l;L,M\rangle\right] \tag{2.45}$$

where the subscript A is included to indicate that the eigenstate is antisymmetric under particle exchange. The factor of $\sqrt{2}$, introduced to preserve the normalization of the states, is only required when $l \neq l'$. When $l = l'$, the normalized angular momentum eigenstates have a different normalization,

$$\begin{aligned} |Q,l^2;LM\rangle_A =& \frac{1}{2}\left[|Q,l^2;L,M\rangle - (-1)^{2l-L}|Q,l^2;L,M\rangle\right] \\ =& |Q,l^2lL,M\rangle \end{aligned} \tag{2.46}$$

One consequence of (2.46) is that, for fermions in the same Landau level, states with certain values of the total angular momentum, L, are non-existent. A pair of fermions with total angular momentum L in the same Landau level necessarily share the same shell angular momentum, l. If we define the relative angular momentum R by the equation $R = 2l - L$, then it is clear that the right side of (2.46) vanishes

when R is even. Equivalently, we can say that fermion triplet pair states with even R are forbidden under all cases. A similar argument using the symmetric analog of (2.46) similarly forbids the formation of fermion singlet pair states with odd R.

2.6 Comparison to other results

In this section, I will verify the expression for the pseudopotential I have derived in equation (2.37) by comparing it to other known results for the pseudopotential.

For the lowest Landau level, also called LL0, it is simplest to compare equation (2.37) to the expression for the pseudopotential on the Haldane sphere given by Fano, Ortolani, and Columbo [G. Fano (1986)] in equation (25) of their paper:

$$V_L^{(Q)} = 2\frac{\begin{pmatrix} 4Q-2L \\ 2Q-L \end{pmatrix}\begin{pmatrix} 4Q+2L+2 \\ 2Q+L+1 \end{pmatrix}}{\begin{pmatrix} 4Q+2 \\ 2Q+1 \end{pmatrix}^2} \tag{2.47}$$

For all tested values of Q and L, equation (2.37) is equal to equation (2.47) divided by $\sqrt{Q}$. The factor of $\sqrt{Q}$ arises from the inclusion of the radius of the sphere, $R_s = \lambda_0\sqrt{Q}$ in (2.37) rather than from a fundamental disagreement. We included the $\sqrt{Q}$ in our expression in order to compare the results on the sphere to those on the plane, which are also given in units of the Coulomb units.

For Landau levels other than the lowest, our expression for the pseudopotential on the Haldane sphere must be compared to the pseudopotentials calculated for electrons on the infinite plane. The pseudopotentials for electrons on a plane are well described in many references [Kivelson et al. (1987); Prange and Girvin (1987)], but I will briefly explain how they can be found here. We begin resolving the particle coordinates into

center of mass and relative coordinates,

$$r_{cm} = \frac{1}{\sqrt{2}}(\mathbf{r}_1 + \mathbf{r}_2) \tag{2.48}$$

$$r_{rel} = \frac{1}{\sqrt{2}}(\mathbf{r}_1 - \mathbf{r}_2) \tag{2.49}$$

The two-body Hamiltonian is separable in the relative and center of mass coordinate systems:

$$H_{cm} = \frac{1}{2\mu}(\mathbf{p}_{cm} + \frac{e}{c}\mathbf{A}_{cm})^2 \tag{2.50}$$

$$H_{rel} = \frac{1}{2\mu}(\mathbf{p}_{rel} + \frac{e}{c}\mathbf{A}_{rel})^2 + \frac{e^2}{r_{rel}} \tag{2.51}$$

The solution for the center of mass coordinates is obviously given by (2.2). To simplify notation for the remainder of this section, expectation values are given in bra-ket notation, where the ket $|N\ M\rangle$ is related to the wavefunction of (2.2) by

$$\langle \mathbf{r}_{cm}|N\ M\rangle = \Psi_{N,M}(r,\phi). \tag{2.52}$$

Here, we will use capital letters for the quantum numbers of the center of mass, and lower case letters for the solutions in relative coordinates. The basis states for the relative coordinates are similarly given by the solutions $|n\ m\rangle$ to (2.51) in the absence of the Coulomb interaction.

The pseudopotentials, $V_{n,m}$ for a pair of particles in the lowest Landau level ($n = 0$) are simply given by the expectation value of the Coulomb interaction in the normalized relative coordinate basis,

$$V_{0,m} = \langle 0m|\frac{1}{r_{rel}}|0m\rangle. \tag{2.53}$$

The pseudopotentials are fully independent of the center of mass.

Table 2.1: Raising and lowering operators acting on single-particle states in the symmetric gauge.

$m \leq 0$	$a^\dagger\|n,m\rangle = \sqrt{(n+1)}\|n+1,m+1\rangle$	$a\|n,m\rangle = \sqrt{n}\|n-1,m-1\rangle$
$m > 0$	$a^\dagger\|n,m\rangle = \sqrt{(n+\|m\|+1)}\|n,m+1\rangle$	$a\|n,m\rangle = \sqrt{(n+\|m\|)}\|n,m-1\rangle$

The pseudopotentials in higher Landau levels are not as simply written because, for example, a pair of electrons in the first excited Landau level have $n_1 = n_2 = 1$, but the center of mass and relative coordinate principle quantum numbers vary between 0, 1, and 2. In order to clarify this problem, we use the appendix of [Kivelson et al. (1987)], and express equation (2.2) in terms of a new set of independent variables,

$$z = \xi e^{-i\phi}, \tag{2.54}$$

$$\bar{z} = \xi e^{+i\phi}. \tag{2.55}$$

Using these new variables, equation (2.2) becomes

$$\begin{aligned} \Psi_{n,m}(z,\bar{z}) &= \mathcal{N}_{n,m} z^{|m|} e^{z\bar{z}/4} L_n^{|m|}(z\bar{z}/2), \text{ for } m \leq 0 \\ \Psi_{n,m}(z,\bar{z}) &= \mathcal{N}_{n,m} \bar{z}^{|m|} e^{z\bar{z}/4} L_n^{|m|}(z\bar{z}/2), \text{ for } m > 0 \end{aligned} \tag{2.56}$$

The raising and lowering operators, $a^\dagger$ and a, respectively, are given by

$$\begin{aligned} a^\dagger &= \sqrt{2}(-\partial_z + \frac{\bar{z}}{4}) \\ a &= \sqrt{2}(+\partial_{\bar{z}} + \frac{z}{4}). \end{aligned} \tag{2.57}$$

They operate on the normalized single particle eigenstates according to table 2.1.

So, in the separated center of mass and relative coordinate basis, the first excited Landau level is not given by $N = 1, n = 1$, but rather by the expression,

$$|\Psi_{LL1}\rangle = a_1^\dagger a_2^\dagger |0M, 0, m>, \tag{2.58}$$

Table 2.2: Pseudopotentials on an infinite plane. The pseudopotentials were calculated using raising and lowering operators in the symmetric gauge for LL0 and LL1. The pseudopotential for LL2 was taken from [Yoshioka (2002)]

m	LL0	LL1	LL2
0	0.88623	0.60928	0.50629
1	0.44311	0.41542	0.36046
2	0.33234	0.45004	0.37334
3	0.27695	0.31503	0.31530
4	0.24233	0.26353	0.33749
5	0.21809	0.23216	0.22642
6	0.19992	0.21014	0.22642
7	0.18564	0.19351	0.20481

where $a_1^\dagger$ and $a_2^\dagger$ are the raising operators for each electron in the independent particle basis, not in the center of mass and relative coordinate basis.

The pseudopotentials for the n^{th} Landau level are defined as the expectation value of the Coulomb potential for two electrons each in Landau level n as a function of their relative angular momentum quantum number m. So, for the first excited Landau level, $n = 1$, and the pseudopotential $V_{n,m}$ is calculated using the following equation:

$$V_{1,m} = \langle 0M, 0m | a_1 a_2 \frac{1}{|z_{rel}|} a_1^\dagger a_2^\dagger | 0M, 0m \rangle. \tag{2.59}$$

Although the center of mass azimuthal quantum number M appears in the above expression, $V_{n,m}$ is independent of M in every Landau level because $1/|z|_{rel}$ operates only on the relative coordinates. The pseudopotentials for the lowest three Landau levels are tabulated in table 2.2; the pseudopotentials for LL0 and LL1 were calculated using the raising and lowering operators in the symmetric gauge for the lowest two Landau levels and agree with [Yoshioka (2002)]; the pseudopotentials from Landau level 2 were not evaluated, and are taken directly from [Yoshioka (2002)].

The derived spherical pseudopotentials can be directly compared to the planar pseudopotentials with a few adjustments. First, the azimuthal quantum number m for a pair of particles in the n^{th} Landau level on the plane is equivalent to a quantity

on the Haldane sphere called the relative angular momentum, R. The relative angular momentum R is given by

$$R = 2l_n - L \tag{2.60}$$

where l_n is the shell angular momentum of the n^{th} Landau level and L is the total angular momentum of the pair.

In addition to being able to compare m on the plane and R on the sphere, it is also necessary to account for the radius of the Haldane sphere. On the Haldane sphere, the pseudopotentials for a given magnetic monopole strength (and therefore spherical radius) are not exactly equal to the pseudopotentials on the plane due to the curvature of the sphere. However, the spherical pseudopotential should approach the planar limit asymptotically in the limit of an infinitely large sphere.

So, to verify the pseudopotentials on the Haldane sphere against planar values, I have evaluated the pseudopotentials given by (2.37) for $Q = 10, 20, \ldots 100$ for several different values of $R = 2l_n - L$ in the first excited Landau level (LL1). In Mathematica, the points for $V(Q, R)$ were fitted by function $f_R(Q) = A + B/Q + C/Q^2$ for different values of R. The limit for each R of the function $f_R(Q)$ for infinite Q matched the planar pseudopotentials to within at least 10^{-5}.

2.7 Finite thickness

Up until this point, I have generally assumed the V_k coefficients of equations (2.3) and (2.37) are those that define the Coulomb potential: that is, $V_k = 1$ for all k. However, any number of other scalar potentials that are functions of $|r_{12}|$, the distance between a pair of particles, can be described by a different choice of the V_k coefficients. One factor that controls the coefficients is the perpendicular containment of the electrons.

In the idealized quantum Hall effect, the electrons are considered to rest in a potential well that is a delta function in the z-direction; that is, they are confined to an infinitely thin, perfectly 2-dimensional potential well. But obviously, in a real system,

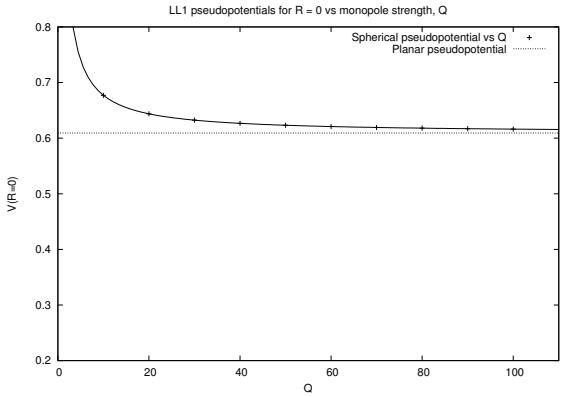

(a) LL1 $V(R=0)$ pseudopotential vs Q

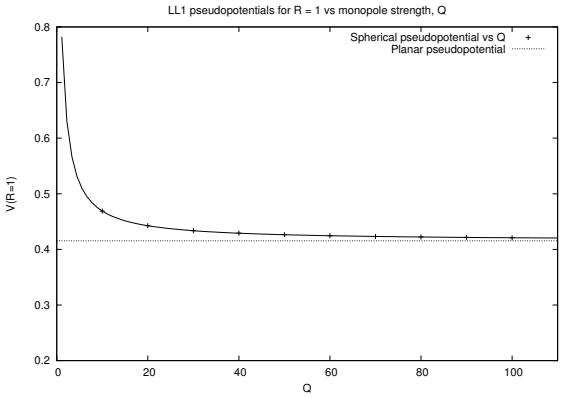

(b) LL1 $V(R=1)$ pseudopotential vs Q

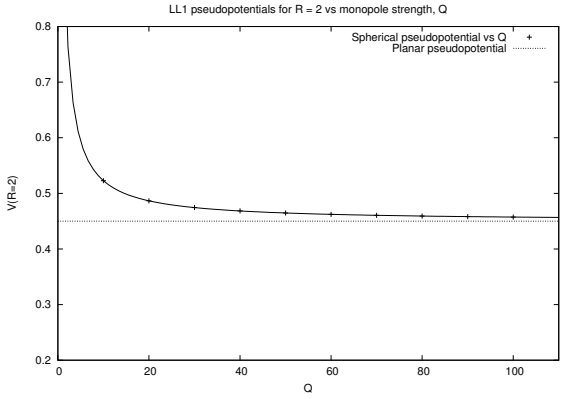

(c) LL1 $V(R=2)$ pseudopotential vs Q

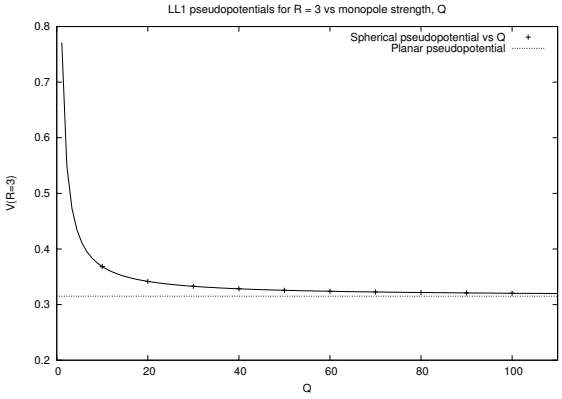

(d) LL1 $V(R=3)$ pseudopotential vs Q

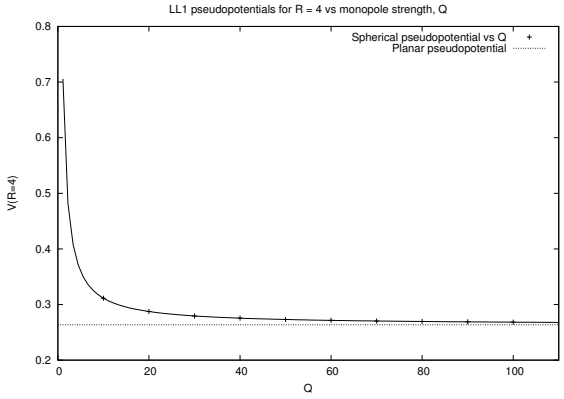

(e) LL1 $V(R=4)$ pseudopotential vs Q

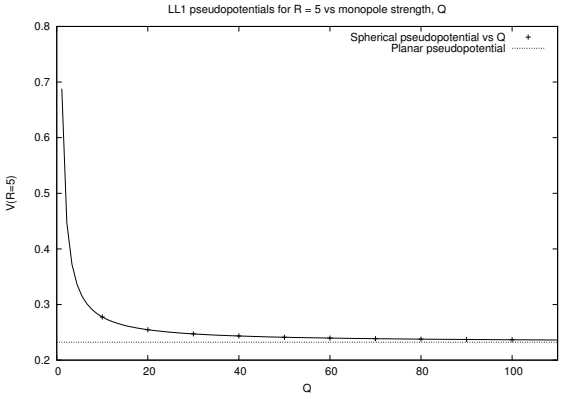

(f) LL1 $V(R=5)$ pseudopotential vs Q

Figure 2.1: Haldane pseudopotentials in the first excited Landau level versus the magnetic monopole strength Q for relative angular momentum $R = 0, 1, \ldots, 5$ calculated using equation (2.37). The horizontal line in each plot gives the pseudopotential evaluated on the two-dimentional plane. As expected, the pseudopotentials in the spherical system are an approximation to the planar pseudopotentials, but approach the planar values in the infinitely large sphere limit.

the electrons are confined by a finitely-thick potential well. For very thin sheets, it is appropriate to consider the i^{th} electron's wavefunction to be the product of the wavefunction along the surface, $\psi(r_i)$ and wavefunction in the direction perpendicular to that surface, $\psi_(z_i)$.

Because the surface is very thin, we can approximate the electron-electron interaction in the actual 3-dimensional system as a modification to the Coulomb interaction in 2-dimensions. The effective two-dimensional Coulomb interaction is found by integrating over the z-direction portion of the two electrons with

$$V(r_{12}) = \iint \frac{|\psi(z_1)\psi(z_2)|^2}{\sqrt{(z_1 - z_2)^2 + r_{12}^2}} dz_1 dz_2. \tag{2.61}$$

The effective two-dimensional interaction, $V(r_{12})$ can then be expanded in Legendre polynomials to give the V_k coefficients used in (2.3) and (2.37),

$$V_k = \frac{1}{2} \int_0^\pi V(r_{12}) P_k(\cos\theta) \sin\theta d\theta. \tag{2.62}$$

For several distinct z-direction confinement potentials, the effect of finite thickness has already been addressed in [Peterson et al. (2008)]. In that paper, the effect of the finite well shapes were evaluated by incorporating the well shape into the Fourier transform definition of the Haldane pseudopotentials and projecting the pseudopotentials into the lowest Landau level.

2.8 Inverse problem

According to the previous section, we can control the behavior of the V_k coefficients by controlling physical properties of system. In particular, I have addressed how the shape of the confining well of the very-thin two-dimensional shell can be adjusted to produce different sets of V_k coefficients, and as a result, different pseudopotentials and correlative behaviors.

One particularly nice feature of our derivations in sections 2.3 and 2.4 is that we can take a desired pair or three-body pseudopotential, and invert the problem to yield a set of desired V_k coefficients that produce the desired behavior. This should be of particular interest to experimentalists because it suggests a possible way of engineering materials that produce the correlations that have been predicted in theoretical models for systems obeying certain pseudopotentials. In addition, the resulting V_k coefficients can be used to extract the form of the actual two-body potential, $V(r_{12})$ from any artificial pair pseudopotential, $V(L)$.

I will first address the simple case of inverting the pair pseudopotentials to yield the V_k coefficients, and will present the inversion for the Laughlin and harmonic pseudopotentials. Finally, we will also consider the more challenging problem of inverting a three-body pseudopotential.

2.8.1 Pair pseudopotential inversion

For electrons confined to the n^{th} Landau level, where the angular momentum shell is defined by $l = Q + n$, we begin with a defined model pseudopotential function, $V_{l,Q}(L)$, and solve (2.37) for the undetermined V_k coefficients,

$$V_{l,Q}(L) = \frac{1}{\sqrt{Q}} \sum_{k=0}^{2l} V_k (-1)^{2Q+L} (2l+1)^2 \begin{Bmatrix} l & l & L \\ l & l & k \end{Bmatrix} \begin{pmatrix} l & k & l \\ -Q & 0 & Q \end{pmatrix}^2 \tag{2.63}$$

The 6J symbols are invariant under any column permutations, and so (2.63) is otherwise identical to (2.37).

The complete pseudopotential function, $V_{l,Q}(L)$ is a set of $(2l+1)$ numbers, with $0 \leq L \leq 2l$ and the shell angular momentum, l, determined by the Landau level $n = l - Q$. So, given a pseudopotential that has been completely enumerated for all allowed values of L, finding the complete set of V_k coefficients means that we only need to solve the linear system of equations in (2.37).

Note that the complete pseudopotential may not be enumerated in all models, and under certain conditions, a number of distinct solutions to the system may give the same pseudopotential behavior. In particular, consider the pseudopotential for a pair of spin-polarized electrons. Ideally, the pseudopotential function would include all integer values of L between 0 and $2l$, but actually, only the pseudopotentials for odd values of the relative angular momentum $R = 2l - L$ determine the electrons' behavior, as shown in section 2.5. The spin polarized electrons' behavior is independent of the even R pseudopotentials values, and substituting set of new values for even R values will not alter the behavior of the electrons at all. However, the alternate pseudopotential spectrum will change the resulting V_k coefficients. In other words, if the pseudopotential defining the electron correlations is either incomplete or non-unique, then the resulting V_k coefficients will not be unique.

Although V_k coefficients can be found by treating (2.63) as a matrix equation and numerically inverting the matrix, the coefficients can also be evaluated directly by making use of the orthogonality property of the Wigner 6J symbols given by equation (6.2.9) in [Edmonds (1996)],

$$\sum_j (2j+1)(2j''+1) \begin{Bmatrix} j_1 & j_2 & j' \\ j_3 & j_4 & j \end{Bmatrix} \begin{Bmatrix} j_3 & j_2 & j \\ j_1 & j_4 & j'' \end{Bmatrix} = \delta_{j',j''} \tag{2.64}$$

In order to use this orthogonality property, we will first exchange the first and third columns of the 6J symbol of equation (2.37).

We then introduce a new varible, j, to(2.63). by multiplying both sides by a function of L and j to yield

$$V_{l,Q}(L)\left[(-1)^{-L}(2L+1)(2j+1)\begin{Bmatrix} l & l & j \\ l & l & L \end{Bmatrix}\right] = \frac{1}{\sqrt{Q}}(2l+1)^2(-1)^{2Q}\sum_{k=0}^{2l}\left[V_k\begin{pmatrix} l & k & l \\ -Q & 0 & Q \end{pmatrix}^2(2L+1)(2j+1)\begin{Bmatrix} l & l & j \\ l & l & L \end{Bmatrix}\begin{Bmatrix} l & l & L \\ l & l & k \end{Bmatrix}\right]. \tag{2.65}$$

Taking the sum of both side of (2.65) over all allowed values of L and applying the orthogonality property of (2.64) gives

$$\sum_{L=0}^{2l}V_{l,Q}(L)\left[(-1)^{-L}(2L+1)(2j+1)\begin{Bmatrix} l & l & j \\ l & l & L \end{Bmatrix}\right] = \frac{1}{\sqrt{Q}}(2l+1)^2(-1)^{2Q}\sum_{k=0}^{2l}\left[V_k\begin{pmatrix} l & k & l \\ -Q & 0 & Q \end{pmatrix}^2\delta_{k,j}\right]. \tag{2.66}$$

The Kronecker delta in (2.66) collapses the sum over k, and the resulting V_j coefficients can be calculated directly as a sum over pseudopotential values times vector coupling coefficients,

$$V_j = \frac{\sqrt{Q}}{(2l+1)^2}\begin{pmatrix} l & k & l \\ -Q & 0 & Q \end{pmatrix}^{-2}(-1)^{2Q}\sum_{L=0}^{2l}\left[V_{l,Q}(L)(-1)^{-L}(2L+1)(2j+1)\begin{Bmatrix} l & l & j \\ l & l & L \end{Bmatrix}\right] \tag{2.67}$$

As a verification of the procedure, we first invert the unmodified Coulomb pseudopotential, evaluated using equation (2.37) for a monopole strength $Q = 30$. As must be the case, all resulting V_k coefficients are equal to 1. Of course, the Coulomb potential is already well known and, for a pair of electrons on a surface,

depends upon the angle between their positions,

$$V(\theta_{12}) = \frac{e^2}{4\pi\epsilon R_s} \frac{1}{\sqrt{2}\sqrt{1-\cos\theta_{12}}}. \tag{2.68}$$

But we can also approximate of the Coulomb potential as a function of θ_{12}, which is analogous to the linear distance between the particles, using on the Haldane sphere using the derived V_k coefficients and (2.11). The derived V_k coefficients and the resulting potential are shown in Figure (2.2). As expected, inverting the Coulomb pseudopotential reproduces $V_k = 1$ for all values of k. The oscillations in the plotted potential are due to the restriction on the sum over k in (2.11). This restriction, in turn, occurs because Q is finite. The oscillations become more suppressed as the size of the sphere, and thus Q, are increased.

While this is obviously a pointless exercise for the familiar Coulomb potential, the method of inverting the pseudopotentials allows us to examine the interaction potential of proposed and model pseudopotentials that are less well known. As an example, we will invert a simple harmonic pseudopotential, a pseudopotential of the form $V_H(L) = aL(L+1) + b$.

It is known [Wójs and Quinn (2000)] that, for any many-body system, a harmonic pseudopotential does not break the energy degeneracy of n-particle angular momentum eigentstates of the same total angular momentum L'. In addition, any linear combination of n-particle angular momentum eigenstates with the same total angular momentum L' will also have the same energy. Because the harmonic pseudopotential does not break the energy degeneracy of the angular momentum eigenstates, it does not introduce electron correlations. Correlations are introduced instead by deviations from the harmonic pseudopotential. For example, pseudopotentials that increase more quickly than $L(L+1)$ are called superharmonic, and cause electrons to preferentially avoid pairings with higher pair angular momenta. Correlations in which electrons avoid pair amplitudes with the highest possible pair angular momenta are known as Laughlin correlations.

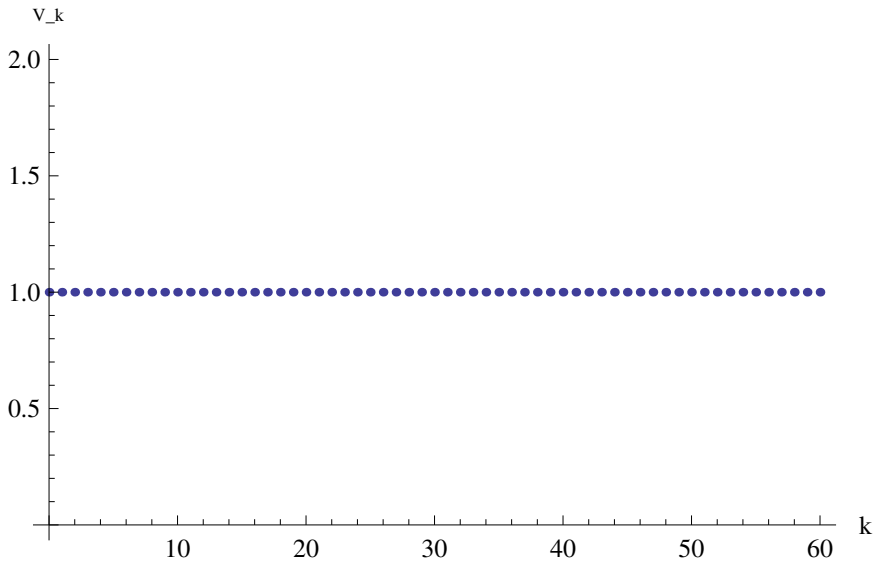

(a) Coulomb V_k coefficients for $Q = 30$ obtained by inverting pseudopotential.

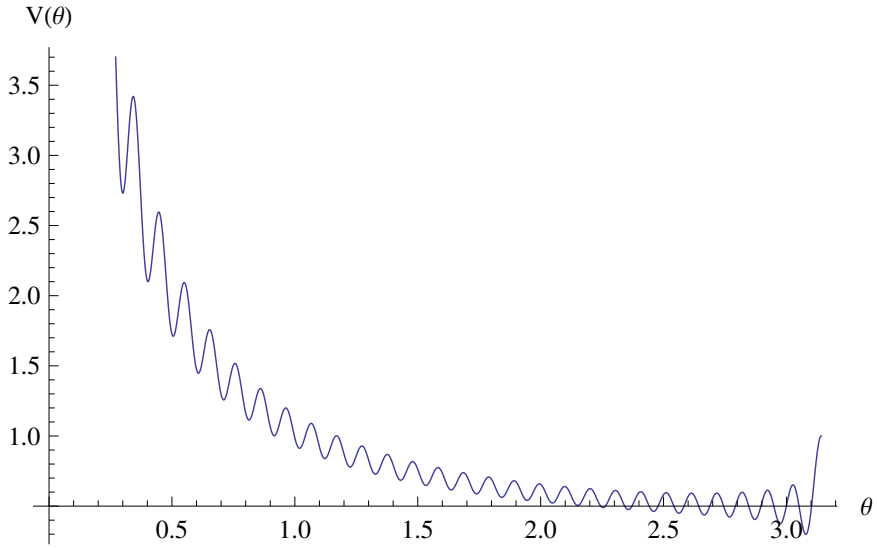

(b) Coulomb potential, $V(\theta_{12})$, for $Q = 30$ obtained by inverting pseudopotential.

Figure 2.2: Coulomb potential, $V(\theta_{12})$, and V_k coefficients for $Q = 30$ obtained by inverting pseudopotential. $V(\theta_{12})$ is given in units of the Coulomb energy, $e^2/4\pi\epsilon\lambda_0$. The V_k coefficients are unitless and are equal to 1 for all values of k, as expected.

We take a simple harmonic pseudopotential given by

$$V_{Q,l}^{Har}(L) = \frac{1}{2l(l+1)\sqrt{Q}} L(L+1), \tag{2.69}$$

where the multiplicative coefficient is a constant that has been chosen to give $V_0 = 1$. Inverting this pseudopotential yields the results shown in figure (2.3) for LL0. The result in LL1 is almost identical to those in LL0: the V_k coefficients for LL0 are all equal to zero, except $V_0 = 1$ and $V_1 = 1.03333$; in LL1, the V_k coefficients are also all equal to zero, except $V_0 = 1$ and $V_1 = 1.1022$. Altering the coefficients a and b of a generic harmonic pseudopotential, $V(L) = aL(L+1) + b$ alters only the values of V_0 and V_1, but leaves all other $V_k = 0$ unchanged. Inverting the pseudopotential makes it clear that, for any harmonic pseudopotential, the interaction potential $V(\theta_{12})$ involves only the monopole and dipole terms of the partial wave expansion. Correlations that occur in the quantum Hall system are instead a function of the higher order terms of the expansion.

Another useful model pseudopotential is the hard-sphere delta pseudopotential, given by a delta function, $V(R) = c * \delta(1 - R)$, where $R = 2l - L$ is the relative total angular momentum. This pseudopotential is the most extreme example of a pseudopotential that produces Laughlin correlations, and the celebrated Laughlin wavefunction is an exact solution to this particular pseudopotential.

Inverting this simple delta function pseudopotential in LL0, however, produces highly oscillatory acting potentials, as shown in figure 2.4. The oscillations are extreme because the V_k values becoming increasingly negative with increasing k, and they obscure the potential's actual nature. Integration of the potential over the relatively small interval $(0, \pi/32)$ yields 87.8% of the total integrand on the interval $(0, \pi)$, and that percentage increases with Q. This behavior suggests that, as Q becomes infinitely large and the Haldane sphere increasingly approximates an infinite plane, the acting potential for the delta pseudopotential is itself a delta function, $V(\theta_{12}) = d * \delta(\theta_{12})$.

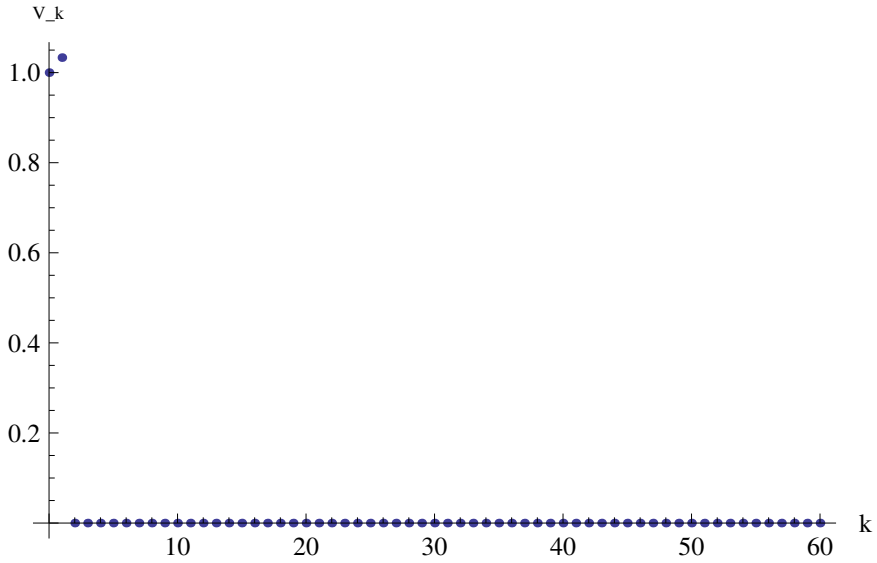

(a) V_k coefficients for the Harmonic pseudopotential in LL0 for $Q = 30$, obtained by inverting pseudopotential.

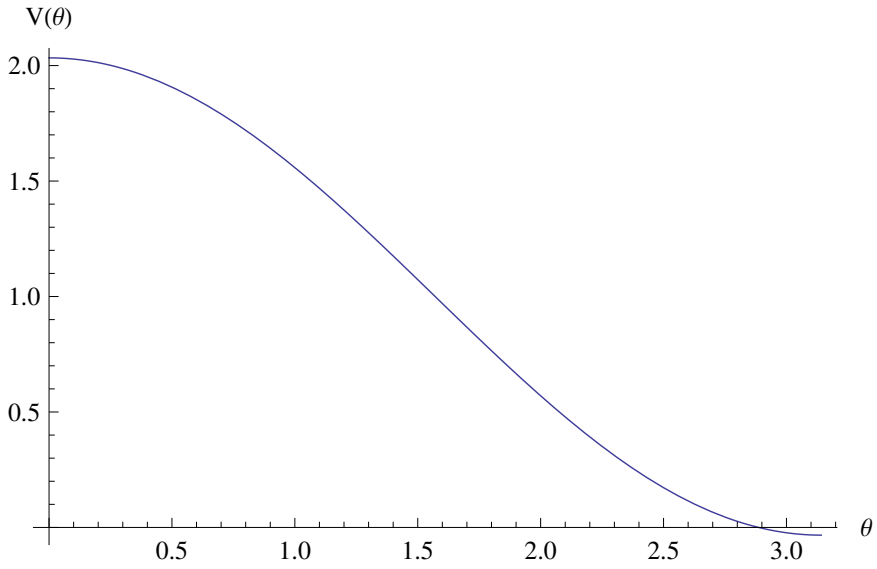

(b) Harmonic potential, $V(\theta_{12})$ in LL0, for $Q = 30$ obtained by inverting pseudopotential.

Figure 2.3: Harmonic potential, $V(\theta_{12})$, and V_k coefficients for $Q = 30$ obtained by inverting a harmonic pseudopotential, $V(L) = a * L(L+1)$, where a is an arbitrary constant defined here by $a^{-}1 = 2l(l+1)\sqrt{Q}$. $V(\theta_{12})$ is given in units of the Coulomb energy, $e^2/4\pi\epsilon\lambda_0$. The V_k coefficients are unitless and are exactly equal to 0 for all values of $k > 1$. In LL0, $V_0 = 1$ and $V_1 = 1.0333$. The result in LL1 are almost identical to those in LL0, except $V_1 = 1.1022$, and are not reproduced here.

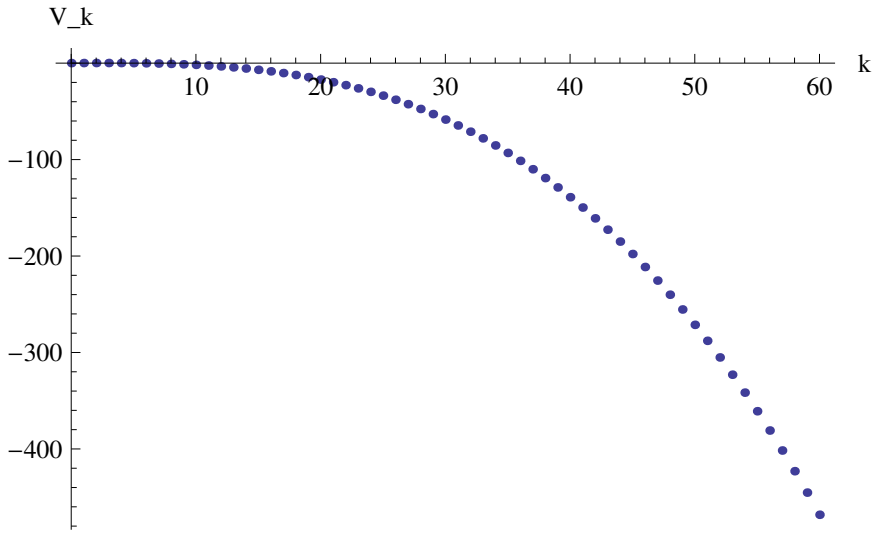

(a) V_k coefficients for a delta function pseudopotential in LL0 for $Q = 30$, obtained by inverting pseudopotential.

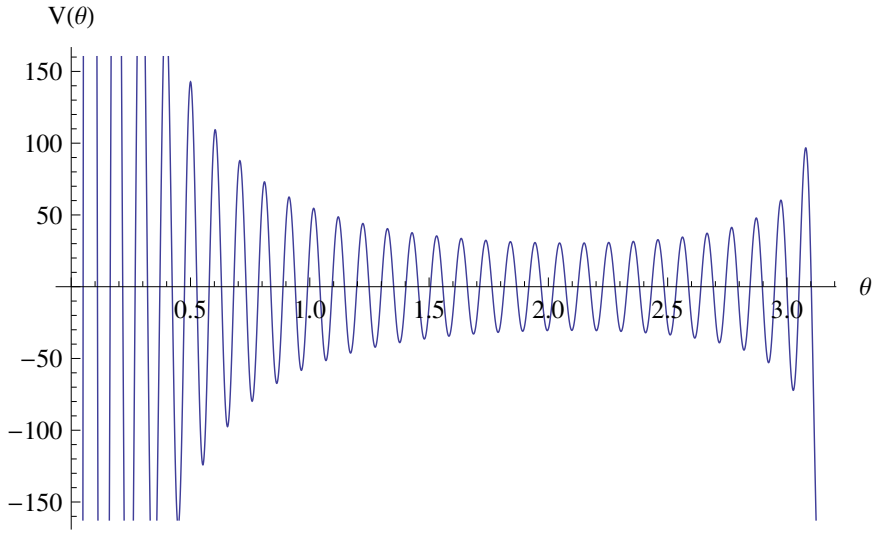

(b) The potential, $V(\theta_{12})$ resulting from a delta function pseudopotential in LL0, for $Q = 30$ obtained by inverting pseudopotential.

Figure 2.4: Delta potential, $V(\theta_{12})$, and V_k coefficients for $Q = 30$ obtained by inverting the pseudopotential $V(L) = a * \delta(2l - 1 - L)$, where a is constant given by $a^-1 = \sqrt{Q}$. $V(\theta_{12})$ is given in units of the Coulomb energy, $e^2/4\pi\epsilon\lambda_0$. The extreme oscillations are due to the increasingly negative values of V_k for larger values of k, and obscure the nature of the potential. Because integration over interval $(0, \pi/32)$ provides 87.8% of the total integrand here, and that percentage increases for larger Q, this potential is best described as an approximation of a delta function in θ_{12}, $V(\theta) = \delta(\theta)$.

The inverted acting potential $V(r_{12})$ and associated V_k coefficients for LL1 are shown in figure (2.5). Unlike in LL0, the delta pseudopotential does not produce a delta function in θ_{12}. Unexpectedly, the predicted potential is actually attractive at very small inter-electron separations.

2.8.2 Three-body pseudopotential inversion

Because the electron-electron interaction is fundamentally a two-body interaction, it is generally most useful to describe the electron correlations in terms of the two-body interactions, either $V(r_{12})$ or the pair pseudopotential $V(L_2)$. However, the electronic behavior is also occasionally given in terms of 3-electron angular momentum energy expectation values,

$$\langle l^3 \alpha' L' M' | V_{123} | l^3 \alpha L M \rangle, \tag{2.70}$$

where $|l^3 \alpha L M\rangle$ is a totally antisymmetric 3-electron eigenstate with total angular momentum L. The monopole strength, Q, has been dropped from the expressions in this section for succinctness and does not affect the calculations. The index α is an arbitrary label introduced to distinguish orthonormal antisymmetric eigenstates with the same total angular momentum.

Invoking the Wigner-Eckart theorem, it is clear that $\langle l^3 \alpha' L' M' | V_{123} | l^3 \alpha L M \rangle$ is diagonal in both L and M, and is also independent of M as long as V_{123} is a scalar.

$$\begin{aligned} \langle l^3 \alpha' L' M' | V_{123} | l^3 \alpha L M \rangle =& (-1)^{L'-M'} \begin{pmatrix} L' & 0 & L \\ -M' & 0 & M \end{pmatrix} \langle \alpha' L' || \mathbf{V} || \alpha L \rangle. \\ =& \frac{1}{\sqrt{2L+1}} \langle \alpha' L' || \mathbf{V} || \alpha L \rangle \delta_{L',L} \delta_{M',M} \end{aligned} \tag{2.71}$$

Although V_{123} is diagonal in L and M, it is not in general diagonal in the index α. Because any number of different angular momentum coupling schemes can be used to construct the set of angular momentum eigenstates, $|l^3 \alpha L M\rangle$ that have the same

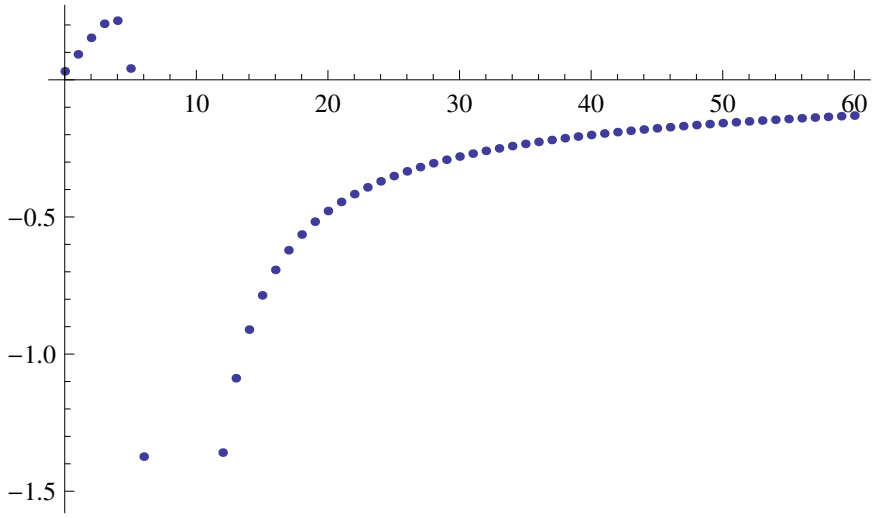

(a) V_k coefficients for a delta function pseudopotential in LL0 for $Q = 30$, obtained by inverting pseudopotential.

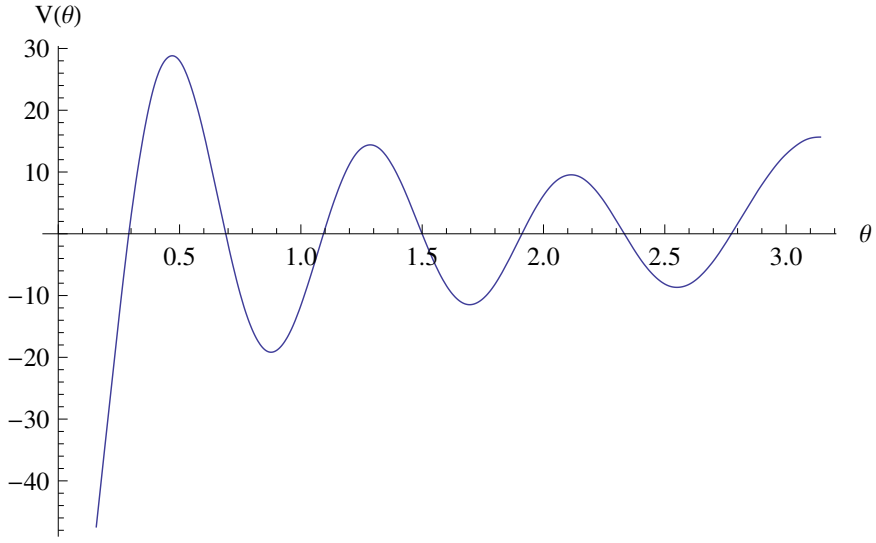

(b) The potential, $V(\theta_{12})$ resulting from a delta function pseudopotential for $Q = 30$ obtained by inverting pseudopotential.

Figure 2.5: Delta potential, $V(\theta_{12})$, and V_k coefficients for $Q = 30$ obtained by inverting the pseudopotential $V(L) = a * \delta(2l - 1 - L)$, where a is normalization constant given by $a^{-}1\sqrt{Q}$. $V(\theta_{12})$ is given in units of the Coulomb energy, $e^2/4\pi\epsilon\lambda_0$. Unlike in LL0, the LL1 delta pseudopotential does not produce a delta function in θ_{12}, but rather a genuinely oscillatory function that is attractive at $\theta = 0$.

L, it is necessary to know their construction if the pseudopotential is not degenerate for all α states with the same L.

To extract the pair pseudopotential $V(L_{12})$ from the 3-body pseudopotential $V(L, \alpha', \alpha)$, we will use the coefficients of fractional parentage, which are defined in [U. Fano (1959)]. The coefficients of fractional parentage are used to express antisymmetric angular momentum eigenstates of n particles as a sum over antisymmetric states of the first $n-1$ particles times the states of the n^{th} particle. In the case of 3 electrons in the same spin shell, the antisymmetric angular momentum eigenstate can be written as

$$|l^3 \alpha L M\rangle = \sum_{\substack{M_{12}, m_3 \\ L_{12}}} |l^2 L_{12} M_{12}\rangle |l m_3\rangle \langle L_{12} M_{12} l m_3 | L_{12} l L M\rangle (l^2 L_{12} l L] \} l^3 \alpha L). \tag{2.72}$$

The angular momentum eigenstate for electrons labeled 1 and 2, $|l^2 L_{12} M_{12}\rangle$, is antisymmetric, and since the electrons share the same spin, exists only for $2l - L_{12}$ an odd integer. The term $\langle L_{12} M_{12} l m_3 | L_{12} l L M\rangle$ is an ordinary Clebsch-Gordan coefficient, and the coefficient of fractional parentage is $(l^2 L_{12} l L] \} l^3 \alpha L)$ in Racah notation. As a shorthand, we will use $(L_{12}] \} \alpha L)$ to represent the complete coefficient of fractional parentage, $(l^2 L_{12} l L] \} l^3 \alpha L)$. Expressions for the explicit evaluation of the coefficients of fractional parentage are given in [Hassitt (1955)].

If the three-particle interaction potential is a sum over two-particle interactions $V_{123} = V_{12} + V_{13} + V_{23}$ for indistinguishable particles labeled 1, 2, and 3, then three-particle matrix element is equal to three times the matrix element of V_{12}:

$$\langle l^3 \alpha' L M | V_{123} | l^3 \alpha L M\rangle = 3 \langle l^3 \alpha' L M | V_{12} | l^3 \alpha L M\rangle. \tag{2.73}$$

Combining (2.72) with (2.73) yields

$$\langle l^3\alpha' LM|V_{123}|l^3\alpha LM\rangle = 3\sum_{\substack{M_{12}m_3L_{12}\\ M'_{12}m'_3L'_{12}}} \langle l^2L'_{12}M'_{12}|V_{12}|l^2L_{12}M_{12}\rangle\langle L'_{12}lLM|L_{12}M_{12}lm_3\rangle$$
$$\langle L_{12}M_{12}lm_3|L_{12}lLM\rangle(\alpha' L\{[L'_{12})(L_{12}]\}\alpha L)\delta_{m_3,m'_3} \tag{2.74}$$

The term $\langle l^2L'_{12}M'_{12}|V_{12}|l^2L_{12}M_{12}\rangle = V(L_{12})$ is simply the pair pseudopotential. Since the Wigner-Eckart theorem applies to the pair pseudopotential term as well, we can introduce $\delta_{L_{12},L'_{12}}\delta_{M_{12},M'_{12}}$ into the equation to simplify it to

$$\langle l^3\alpha' LM|V_{123}|l^3\alpha LM\rangle = 3\sum_{M_{12},m_3,L_{12}} V(L_{12})\langle L_{12}lLM|L_{12}M_{12}lm_3\rangle$$
$$\langle L_{12}M_{12}lm_3|L_{12}lLM\rangle(L\alpha\{[L_{12})(L_{12}]\}L\alpha) \tag{2.75}$$

Including the unitary property of the Clebsch-Gordan coefficients, [Edmonds (1996)] equation (3.5.4), equation (2.75) simplifies the sum over M_{12} and m_3 to give

$$\langle l^3\alpha' LM|V_{123}|l^3\alpha LM\rangle = 3\sum_{L_{12}} V(L_{12})(\alpha' L\{[L_{12})(L_{12}]\}\alpha L). \tag{2.76}$$

Equation (2.76) cannot be analytically inverted because the coefficients of fractional parentage do not form a complete unitary set because they are the coefficients that diagonalize a projection operator. Instead, the linear system of (2.76) should be inverted numerically.

Inverting (2.76) numerically is not entirely straigtforward: because the number of allowed antisymmetric L_{12} values is smaller than the number of allowed antisymmetric 3-body states, $|l^3\alpha L\rangle$ for a given M, the linear system of equations in (2.76) is in general overdetermined. Even if we artificially include the even values of $R_{12} = 2l - L_{12}$ in the sum to increase the number of variables on the right side of (2.76), for $l \geq 5$, there are more state vectors $|l^3L\alpha\rangle$ on the left side of the equation than there are

integer values of $L_{12} < 2l$. As a result, there exist trial 3-body pseudopotentials that cannot be inverted to give a consistent two-body pseudopotential that is the result of a scalar two-body interaction, $V(r_{12})$.

Chapter 3

N-particle solutions, numerical methods

The calculation of two-body interactions in the quantum Hall system was covered in Chapter 2, but in general we are interested modeling the behavior of systems with rather more than two electrons. It is the collective behavior of many electrons that defines the fractional quantum Hall effect, and that collective behavior can be calculated numerically through exact numerical diagonalization. Essentially, calculations of this type constitute numerical experiments for evaluating the validity of proposed trial wavefunctions predicting the collective behavior electrons in the experimental quantum Hall system. In particular, these numerical experiments provide a way to test trial wavefunctions in the absence of a method of directly measuring the wavefunction amplitudes in a physical experimental system.

In the following sections, I will review the methods and assumptions necessary to study the N-body problem in using configuration interaction calculations. Although the quantum Hall effect is a discovery based in condensed matter physics, the most common computational techniques and theoretical framework used to evaluate the many-body energies and wavefunctions are more commonly associated with atomic and chemical physics. In particular, the Haldane sphere model is particularly

suited to being treated as an atomic-like system, and as such, it is relatively straightforward to solve the problem using Slater determinants and configuration interaction calculations, both of which will be reviewed below.

After presenting some numerical results, I will also derive a method for directly calculating the coefficients of fractional parentage in this same framework.

3.1 Configuration interaction calculations

The n-electron problem on the Haldane sphere consists of finding the lowest energy eigenvalues and corresponding n-electron eigenvectors of the Schrödinger equation with the Hamiltonian

$$\hat{H} = \sum_i \hat{H}_{0,i} + \frac{e^2}{4\pi\epsilon} \sum_{i<j} \frac{1}{r_{i,j}}. \tag{3.1}$$

Here $\hat{H}_{0,i}$ is the single particle Hamiltonian for the Haldane sphere, given in equation (2.6); it's eigenfunctions are the monopole harmonics described in section 2.2. The complete set of monopole harmonic functions with the same magnetic quantum number Q spans the complete single particle Hilbert space of the quantum Hall problem, but solving the problem in an infinite Hilbert space is impractical. Fortunately, the problem can be simplified by restricting the problem to an appropriate non-infinite Hilbert subspace. The choices of restriction will be discussed in the following section; for now, we assume a restriction to a Hilbert subspace that is spanned by a finite set of N linearly independent single-particle wavefunctions, $\mathcal{S} = \{\phi_1, \phi_2, \ldots, \phi_N\}$. The single-particle wavefunctions are written as ϕ_j, where j is the index of the j^{th} function in the ordered set $\mathcal{S}$. The choice of ordering of these wavefunctions is arbitrary, but some ordering must be defined. If spin is included in the problem, the single particle wavefunctions will include spin functions, χ_j, in addition to spatial wavefunctions.

We can construct totally antisymmetric n-electron wavefunctions called Slater determinants from n-element subsets of $\mathcal{S}$. Let us take $\mathcal{F} = \{\phi_{f1}, \phi_{f2}, \ldots, \phi_{fn}\}$ to be

some arbitrary n-element subset of $\mathcal{S}$, where the elements of $\mathcal{F}$ preserve the ordering of $\mathcal{S}$. Then $\mathcal{F}$ corresponds to a Slater determinant given by:

$$\Phi_{\mathcal{F}}(x_1, \ldots x_n) = \frac{1}{\sqrt{n!}} \begin{vmatrix} \phi_{f1}(x_1) & \phi_{f1}(x_2) & \cdots & \phi_{f1}(x_n) \\ \vdots & \vdots & & \vdots \\ \phi_{fn}(x_1) & \phi_{fn}(x_2) & \cdots & \phi_{fn}(x_n) \end{vmatrix}. \tag{3.2}$$

where x_j is the coordinate of the j^{th} electron. The same Slater determinant can also be written in second quantized notation as

$$|l_1, m_1; l_2, m_2; \ldots; l_n, m_n\rangle = c^\dagger_{l_n,m_n} \ldots c^\dagger_{l_2,m_2} c^\dagger_{l_1,m_1} |0\rangle. \tag{3.3}$$

The creation operator $c^\dagger_{l_i,m_i}$ creates an electron in the single-particle state $|Q, l_i, m_i\rangle$, where the monopole strength Q has been dropped for brevity since, as always, it has the same value for all particles in the system. Each of the $|Q, l, m\rangle$ monopole harmonics maps to a distinct wavefunction in the set $\mathcal{S}$.

The set of all possible n-electron distinct Slater determinants built from $\mathcal{S}$ spans the n-particle Hilbert space of the problem. These Slater determinants are the basis set for diagonalizing the interaction matrix with elements

$$\langle \Phi_a | \hat{H} | \Phi_b \rangle. \tag{3.4}$$

The matrix elements of the matrix are simple to compute using the well-developed rules of Slater determinant formalism, which are described in [Friedrich (2006)] and are derived explicitly in [Bethe and Jackiw (1986)]. The matrix elements can be calculated simply in either of two ways. The first is to evaluate them directly using equation (2.3). The second method, which is used in the majority of publications, is to evaluate two-body interaction terms using the pseudopotential expansion of equation (2.25) with the desired pseudopotential.

Diagonalizing the Hamiltonian matrix in this Slater determinant basis set gives a good approximation to the exact energies and wavefunctions of the experimental system.

3.2 Hilbert subspace

Because any n-body, totally antisymmetric wavefunction can be written as a linear combination of Slater determinants, the eigenvectors of the configuration interaction calculation would be exact solutions to Hamiltonian if the Slater basis states were to span the complete Hilbert space. Unfortunately, spanning the quantum Hall Hilbert space requires an infinite basis set, and so exact numerical solutions are unattainable. The problem can be solved, however, within subspaces of the Hilbert space that can be spanned by a finite set of wavefunctions. If we choose appropriate restrictions to the Hilbert subspace, then the numerical solutions will be very good approximations to the exact solutions for the system.

In the quantum Hall problem, it is most common to restrict the Hilbert subspace to a single, spin-aligned Landau level. This restriction to the Hilbert subspace is a reasonable approximation to the functional space seen by electrons in the quantum Hall system when the magnetic field is exceptionally strong. In this case, the noninteracting single-particle energies within a single Landau level are highly degenerate, but are radically different from the energies of other Landau levels, so it is reasonable to assume that electron excitations to other Landau levels are difficult and rare. In addition, the restriction assumes that a strong enough magnetic field will act to align all of the electron spins and essentially forbids spin flips in the interactions. Calculations performed in this restricted subspace are excellent at predicting the formation of the incompressible quantum liquid states observed experimentally, and are often used as numerical experiments to compare to ansatz wavefunctions.

This usual choice of Hilbert space restriction obviously ignores the possibility of inter-Landau level electron excitations, but the inclusion of more than one Landau

level in numerical calculations is computationally too large to consider for all but the the smallest systems (few electrons and very small Q). We will address electron excitations and Landau level mixing in Chapter 4.

3.3 The Wigner-Eckart theorem

Even though the isolated Landau level approximation greatly reduces the size of the Slater determinant basis set, the problem still grows dramatically with the number of electrons and the size of the Haldane sphere (which is related to Q). The size of the matrix to be diagonalized can be reduced significantly by using the Wigner-Eckart theorem to evaluate the matrix elements.

The matrix element of a spherical tensor operator T^k_q with respect to arbitrary angular momentum eigenstates $|\gamma, j, m\rangle$ is given by the Wigner-Eckart theorem, [Edmonds (1996)] equation (5.4.1):

$$\langle \gamma' j' m' | T^k_q | \gamma j m \rangle = (-1)^{j'-m'} \begin{pmatrix} j' & k & j \\ -m' & q & m \end{pmatrix} \langle \gamma' j' || \mathbf{T}^k || \gamma, j \rangle. \tag{3.5}$$

The reduced matrix element, $\langle \gamma' j' || \mathbf{T}^{(k)} || \gamma, j \rangle$ is independent of the azimuthal quantum numbers m and m', and of the tensor index q. If the tensor operator is a scalar (as is the case for the Coulomb potential), the spherical tensor is of rank 0, and (3.5) simplifies to

$$\langle \gamma' j' m' | T^0_0 | \gamma j m \rangle = (-1)^{j'-m'} \begin{pmatrix} j' & 0 & j \\ -m' & 0 & m \end{pmatrix} \langle \gamma' j' || \mathbf{T}^0 || \gamma, j \rangle \delta_{m,m'} \delta_{j,j'}. \tag{3.6}$$

The Kronecker deltas have been explicitly added to equation (3.6), but are simply properties of the Wigner 3J symbols.

A simple reduction to the problem size comes from the Kronecker delta in the total azimuthal angular momentum M. Because the Slater determinants are

all eigenvectors of the total azimuthal quantum number, $M = \sum m_i$, equation (3.6) applies to the total M even though the Slater determinants are simultaneous eigenstates of the total angular momentum squared, L^2. As a result, the Hamiltonian matrix described in section 3.1 is actually block diagonal in M, and the eigenvalues of each subblock are independent of M. So, instead of diagonalizing the full interaction Hamiltonian, it is more useful to diagonalize only the largest M subblock, the one that includes the maximum number of L eigenstates. The largest of the subblocks, the one which includes all possible total angular momenta L, is the one with the minimum value of $|M|$.

In other words, the Hamiltonian matrix can be reduced in size without loosing any eigenvalues simply by restricting the Hilbert space to that of a single total M. That is, we can reduce the size of the computational problem simply by eliminating all Slater determinants with $\sum m_i \neq 0$ (or $\sum m_i \neq 1/2$ for systems in which n and $2l$ are both odd) without loosing any solutions.

In order to further reduce the matrices to be diagonalized, we can rotate the Slater determinant basis into the coupled angular momentum representation basis via a simple linear transformation,

$$\Psi_{L,M,\alpha} = \sum c_i \Psi_i, \tag{3.7}$$

where Ψ_i are the n-particle Slater determinants and $\Psi_{L,M,\alpha}$ is an angular momentum eigenstate. The index α is an index that distinguishes different orthogonal states with the same total angular momentum, L in the coupled angular momentum representation. If the original Slater determinant basis set spanned a complete subspace of the total angular momentum, then the new angular momentum basis also spans the Hilbert subspace, and the Hamiltonian interaction matrix will yield equivalent solutions even though the matrix elements will obviously be different.

In the new, rotated basis, it is clear that (3.6) implies that the Hamiltonian matrix is block diagonal in both the total angular momentum, L, and the total azimuthal

angular momentum, M. As before, the matrix elements are also independent of M, so we can choose a single value of M to reduce the entire problem. In addition, in the coupled angular momentum representation, the energy spectrum as a function of L can be found by separately diagonalizing separate L subblocks.

In some cases it will prove valuable to rotate the Slater determinant basis into the coupled angular momentum basis before numerical diagonalization, but it is not necessary to resolve the Slater determinants into angular momentum eigenstates prior to diagonalization. Because the Coulomb interaction Hamiltonian can be block diagonalized in L and M, it must be the case that diagonalizing the Hamiltonian in the uncoupled Slater determinant representation yields energy eigenvectors that are also eigenstates of L and M. Essentially, the Wigner-Eckart theorem grants us some flexibility in solving the problem: we can diagonalize the problem over a complete set of Slater determinants, or a set of Slater determinants restricted to a single M. Or, if the problem is particularly large, we can even diagonalize the same problem in the basis set consisting of sums of the Slater determinants that are also eigenstates of the angular momentum. All three methods will give the same solutions.

3.4 Numerical diagonalization

In this section, I will present the results of a few numerical trials for 8 particle systems in the lowest Landau level (LL0) interacting under the unmodified Coulomb potential and discuss the results in connection with the Laughlin state heirarchy and the composite fermion picture. The numerical diagonalizations were performed using LAPACK, or when the matrix was particularly large and sparse, ARPACK.

The Laughlin states occur when $\nu = 1/m$, where m is an odd integer, and they are found on the Haldane sphere in the lowest Landau level (LL0) for an N electron system at $2Q = m(N-1)$. (In this section, the number of electrons is indicated with a capital N in order to distinguish it from the Landau level index, n.) Naively, a $\nu = 1/m$ filling factor on the Haldane sphere should be expected to occur when

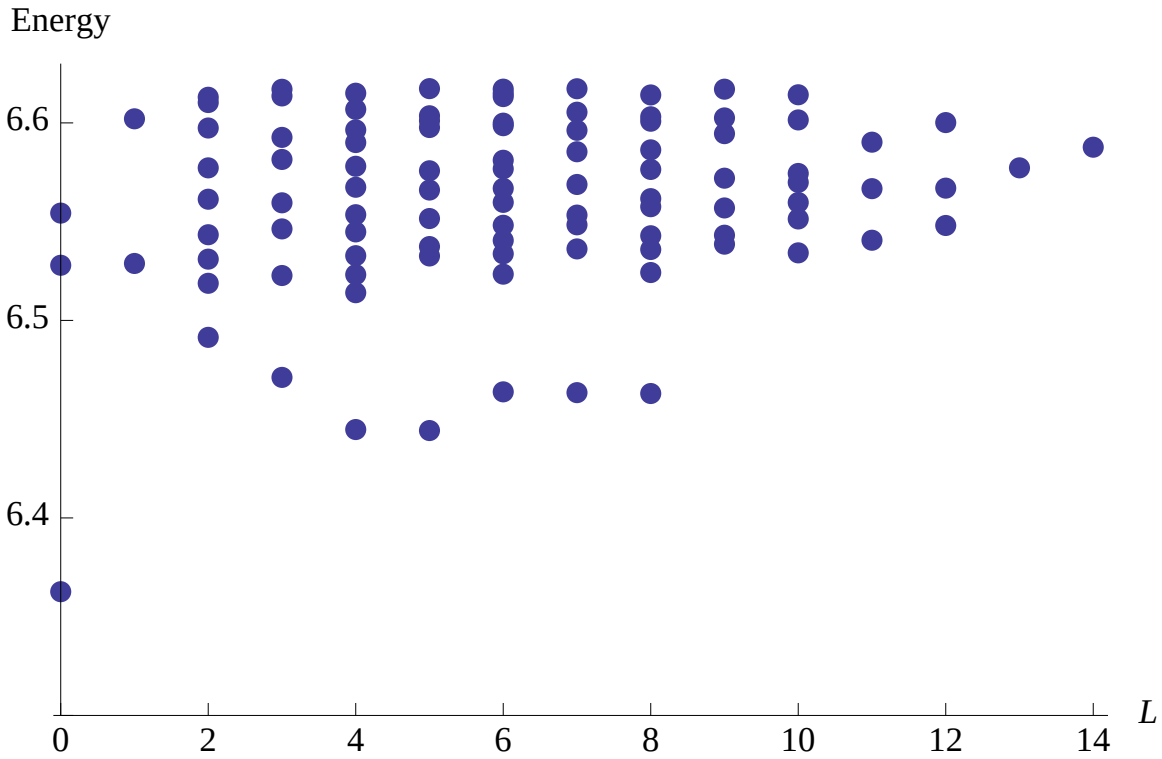

Figure 3.1: Numerical results for $\nu = 1/3$ quantum hall system for 8 electrons and $Q = 21/2$. The ground state at $L = 0$ is the Laughlin incompressible ground state and can be clearly seen with a large energy gap characteristic of the robust $\nu = 1/3$ state. Above the ground state, the low-lying energy band is the energy spectrum of a quasielectron-quasihole pair.

$N/(2Q + 1) = 1/m$. For systems that are numerically practical (meaning N is less than 20 and is usually closer to 10), the incompressible state occurs at the corrected $2Q = m(N - 1)$ rather than the naively determined $2Q = mN - 1$, but the spherical system correction is irrelevant in the limit as N and Q become significantly larger. The energy spectrum for an 8 electron, $\nu = 1/3$ system is presented as a function of the total angular momentum L in figure 3.1. The Laughlin incompressible quantum liquid state is the non-degenerate $L = 0$ ground state, and its stability is marked by a relatively large energy gap. The low-lying energy band above the ground state consists of the excited states with a quasielectron and a quasihole.

If the filling factor is close to, but slightly different from $1/m$, then quasiparticles will form in the quantum Hall system: if $\nu > 1/m$, the quasiparticles will be

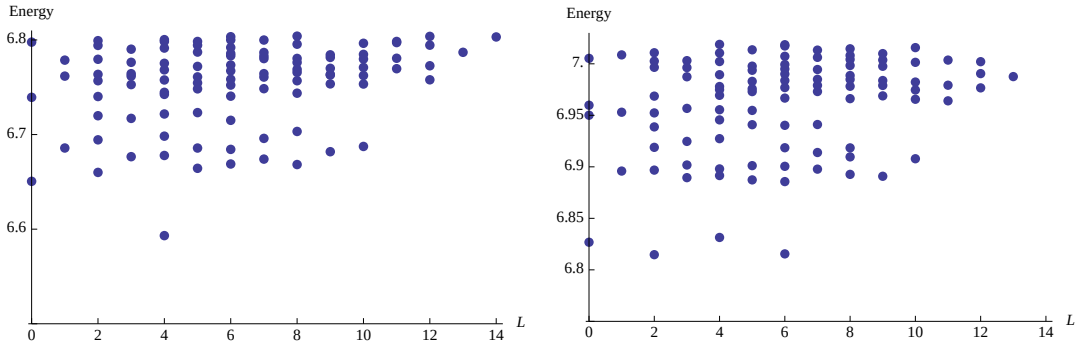

(a) Energy spectrum for $N = 8$ electrons, $Q = 20/2$, near $\nu = 1/3$ filling.

(b) Energy spectrum for $N = 8$ electrons, $Q = 19/2$, near $\nu = 1/3$ filling.

Figure 3.2: The lowest 100 energy eigenvalues near $\nu = 1/3$ filling for 8 electrons ($\nu = 1/3$ occurs at $Q = 21/2$, and is shown in Figure 3.1). When $Q = 20/2$, in shown in 3.2a, the $L = 4$ ground state is a state with a single quasielectron excitation. Figure 3.2b shows the numerical results for $Q = 19/2$. The lowest energy band is the energy spectrum of a pair of quasielectrons. The higher energies correspond to states with multiple quasielectron and quasihole excitations.

quasielectrons; if $\nu < 1/m$, they will be quasiholes. Numerically, for example, the lowest energy state in figure 3.2a is the Laughlin incompressible state plus a single quasielectron. Haldane predicted that, at correct values of ν near the Laughlin parent state, these quasiparticles could themselves form a daughter state that is also incompressible state [Haldane (1983)]. Quasiparticles of the daughter state could then also subsequently form additional incompressible, etc..., producing a hierarchy of possible Laughlin daughter state filling factors. Only a small subset of the Laughlin hierarchy states are actually observed experimentally, and these states are predicted in the Jain composite fermion picture 3.2a [Jain (1989)].

Under the Jain composite fermion picture in the spherical geometry, the total number of magnetic fluxes seen by the electrons is given by $2Q$. Attaching an even number, α, of magnetic flux tubes to each electron transforms each of them into what is called a composite fermion. The effective magnetic monopole strength seen by each composite fermion (CF) is equal to

$$2Q^* = 2Q - \alpha(N - 1). \tag{3.8}$$

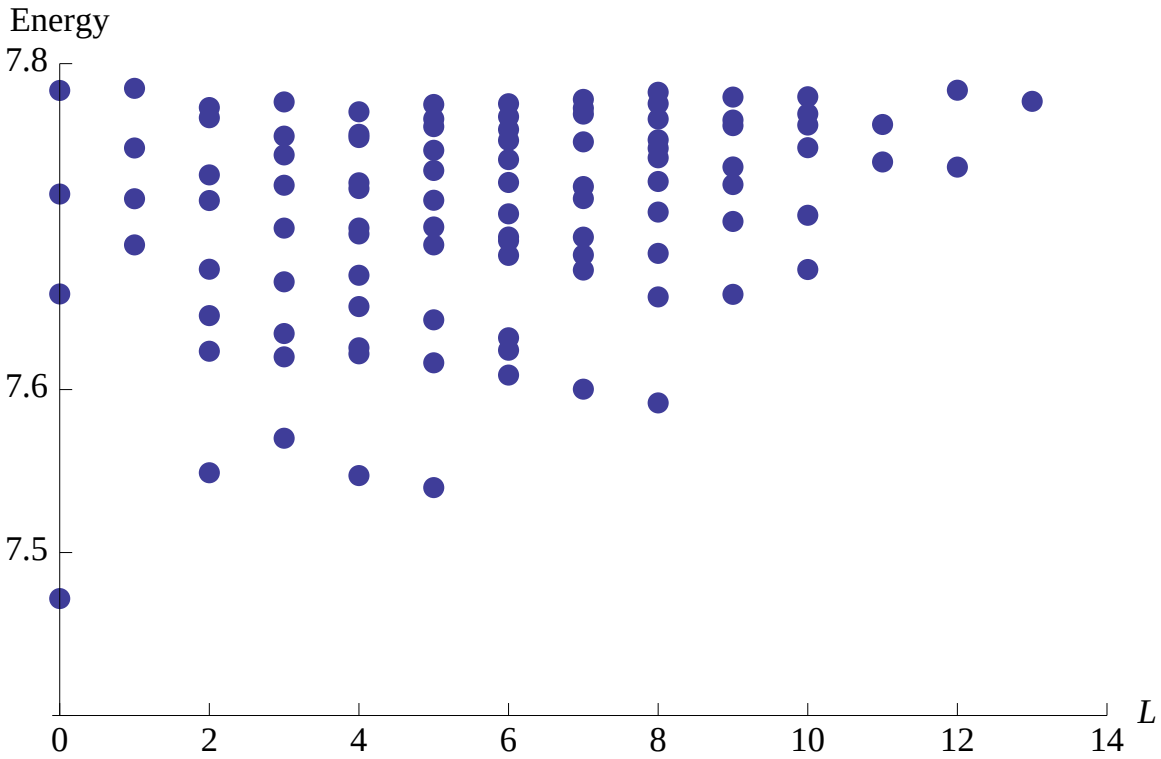

Figure 3.3: Numerical trials for $\nu = 2/5$ quantum Hall system for 8 electrons and $Q = 16/2$. The ground state at $L = 0$ is the incompressible Jain state found at $\nu = 2/5$. The low-lying energy band above the $L = 0$ ground state corresponds to the states of a single quasielectron-quasihole pair.

The effective monopole strength seen by one CF is reduced from $2Q$ by the number of flux tubes per electron, α, times the number of CFs other than itself. This effective monopole strength, $2Q^*$, defines the CF Landau levels, where the n^{th} CF Landau is defined by the angular momentum shell $l_n^* = Q^* + n$ for $n = 0, 1, \ldots$.

An incompressible quantum Hall state occurs when the number of composite fermions exactly fills one or more of these CF Landau levels. For example, let us consider a system with N composite fermions filling only the lowest CF Landau level. Since the Landau level degeneracy is equal to $2l_0^* + 1$, the effective monopole strength must be given by $2Q^* = N - 1$. The total magnetic monopole strength for the system is determined from equation (3.8) to be given by

$$2Q = (\alpha + 1)(N - 1). \tag{3.9}$$

Selecting Q and n and an even value of α to satisfy (3.9) and gives the Laughlin sequence with filling factor $\nu = 1/(1+\alpha)$. The ground states of this sequence consist of a totally filled lowest CF Landau level that is non-degenerate, is incompressible, and has a total angular momentum of $L = 0$. The results of numerical diagonalization for $N = 8$ and $Q = 21/2$ in figure 3.1, which corresponds to the $\nu = 1/3$ state clearly show the $L = 0$ ground state predicted by the CF picture.

When the value of $2Q$ is very close to an incompressible quantum liquid state, quasielectrons or quasiholes will form in the composite fermion shell. When $2Q^* + 1$ is smaller than the number of particles, N, then quasielectrons will be formed in the lowest unoccupied CF shell. For example, in the 8 particle system near $\nu = 1/3$, a monopole strength of $Q = 20/2$ results in ground state with a single quasielectron in the first excited CF Landau level. The value of Q^* is 3 according to equation (3.8). The lowest energy state, which consists of a totally filled CF LL0 and a single quasielectron in the CF LL1, then, has a total angular momentum equal to 4, as can be seen in figure 3.2.

Other sequences of fractional fillings can be produced by filling more than one CF Landau level. For example, the $\nu = 2/5, 2/7, \ldots$ sequence of Jain states results from filling the lowest two CF Landau levels, and occurs when

$$2Q = \frac{2\alpha + 1}{2} n - (2 + \alpha). \tag{3.10}$$

The incompressible $L = 0$ ground state for the $\nu = 5/2$ state can be seen clearly in figure 3.3.

As good as the Jain composite fermion picture is at predicting which of the Laughlin hierarchy states are experimentally (and numerically) observed, the physics of the model cannot be an accurate picture of the dynamics, as discussed in chapter 1. Instead, the existence of a Laughlin incompressible state can be predicted by the interaction pseudopotential of its constituent fermions. A Laughlin incompressible ground state of interacting fermions will occur only when the pseudopotential of

those particles is superharmonic: the pseudopotential must increase faster than a harmonic pseudopotential, $V_H(L) = A + B * L(L+1)$ [Wójs and Quinn (2000)]. In the lowest Landau level, the electron pseudopotential is strongly superharmonic, and as a result, the base Laughlin sequence of $\nu = 1/m$ is strongly observed.

The pseudopotentials for quasielectrons near Laughlin filling factors, however, are not universally superharmonic. The pseudopotential of the quasiparticles can be found numerically by diagonalizing finite systems with pairs of quasiparticles. The resulting lowest energy band is the interaction energy of the pair of quasiparticles as a function of their pair angular momentum, the quasiparticle pseudopotential. The quasielectron pseudopotential of the $\nu = 1/3$ is the lowest energy band shown in figure 3.2b If the quasiparticle pseudopotential is itself superharmonic, then the quasiparticles of the Laughlin parent state can themselves form an incompressible Laughlin state. Pseudopotentials that are not superharmonic induce particle pairing instead of incompressible quantum liquid states. As shown in [Wójs and Quinn (2000)], the pseudopotential description of Laughlin condensation explains the success of the Jain composite fermion states with a more realistic physical picture.

3.5 Pair probabilities and coefficients of fractional grandparentage

In addition to giving the angular momentum dependent energy eigenvalues, exact numerical diagonalization also provides a numerical approximation to the exact many-body wavefunctions of the system. As such, we can use numerical diagonalization studies to directly examine the correlated behavior of electrons in the system in a way that physical experiments do not allow.

In this section, I will cover the coefficients of fractional grandparentage and the pair probabilities, another set of tools useful for analyzing the correlated behavior of electrons. We begin with an n-electron wavefunction that is an eigenfunction of

the square of the total angular momentum, L^2. For this problem, we will assume all electrons are confined to the same Landau level. Because the set of all Slater determinants corresponding to that Landau level spans the n-particle wavefunction Hilbert space, the angular momentum eigenfunction can be written as a sum over Slater determinants:

$$\Psi_{LM\alpha}(x_1, x_2, \ldots, x_n) = \sum c_i \Phi_i(x_1, x_2, \ldots, x_n) \tag{3.11}$$

Here, x_i is shorthand for the full position and spin label of the electrons, $(\mathbf{r}_i, m_{s,i})$. Because the magnetic quantum number Q is unchanged in all parts of the quantum Hall problem, it has been dropped from the expressions in this section. The index α is, as before, a label to distinguish orthogonal wavefunctions that have the same total angular momentum quantum numbers L and M; it represents the complete angular momentum coupling scheme of the angular momentum eigenstate. In general, $\Psi_{LM\alpha}(x_1, x_2, \ldots, x_n)$ can be any n-body angular momentum eigenstate, but the states of interest in this problem are naturally those that are also the energy eigenstates of the quantum Hall problem.

The state vector of the n-electron angular momentum wavefunction can also be written as a coupled angular momentum eigenstate,

$$|\Psi_{LM\alpha}(1, 2, \ldots, n)\rangle \equiv |l^n; LM\alpha\rangle. \tag{3.12}$$

The state vector is fully antisymmetric under the interchange of any pair of electrons. It is an element of the irreducible tensorial set of angular momentum eigenvectors, written $(1, 2 \ldots n]\}l^n, \alpha L\}$, which has $2L + 1$ members. In the notation of Fano and Racah [U. Fano (1959)], the members of the irreducible tensorial set are indicated to be antisymmetrized over particles $1, 2, \ldots, n$ by the symbol "]}" preceded by a list of the particle labels over which the member functions are antisymmetrized.

The same wavefunctions can be constructed from the products of 2-particle and $(n-2)$-particle states using the coefficients of fractional grandparentage. Consider the 2-particle, totally antisymmetric angular momentum eigenstate $|\Psi_{L_{12}M_{12}}(1,2)\rangle \equiv |l^2; L_{12}M_{12}\rangle$ with electrons with labels 1 and 2. It is a member of the irreducible tensorial set $(12]\}l^2L_{12}\}$. Similarly, the totally antisymmetric angular momentum eigenstates of the remaining electrons, with labels $3, 4, \ldots, n$, given by $|\Psi_{L'M'\alpha'}(3,4,\ldots,n)\rangle \equiv |l^{n-2}; L'M'\alpha\rangle$ for all allowed values of M', are members of the antisymmetrized irreducible tensorial set, $(3\ldots n]\}l^{n-2}\alpha'L'\}$. These two irreducible tensorial sets can be coupled to a set of states with total angular momentum L by taking their irreducible product,

$$(12\ldots n|l^nL\} = \left[(12]\}l^2L_{12}\} \times (3\ldots n]\}l^{n-2}\alpha'L'\}\right]^{[L]} \tag{3.13}$$

Note that the expression on the left of equation (3.13) lacks the Fano antisymmetrization symbol, "]}". This is because, although $(12\ldots n|l^nL\}$ is antisymmetric over the interchange of particles 1 and 2 and over the interchange of the other $n-2$ particles, it is not yet antisymmetric over the interchange of particles 1 and 2 with particles $3, \ldots, n$.

Equation (3.13) can be be antisymmetrized to construct the fully antisymmetric set $(12\ldots n]\}l^n; \alpha L\}$ by using the coefficients of fractional grandparentage, which are denoted $G_{L\alpha,L'\alpha'}(L_{12})$ as follows:

$$(12\ldots n]\}l^n; \alpha L\} = \sum_{L_{12}} \sum_{L',\alpha'} G_{L\alpha,L'\alpha'}(L_{12}) \left[(12]\}l^2L_{12}\} \times (3\ldots n]\}l^{n-2}\alpha'L'\}\right]^{[L]}. \tag{3.14}$$

Like the coefficients of fractional parentage described in section 2.8.2, the coefficients of fractional grandparentage are the eigenvector coefficients of the non-zero eigenvalues of the antisymmetrization operator.

In addition to being useful in constructing fully antisymmetric eigenstates of the angular momentum, the coefficients of fractional grandparentage also contain

information about the relative prevalence of electron pairs in the state with a given coupled pair angular momentum, L_{12}. The probability $P_{L\alpha}(L_{12})$ that a given angular momentum eigenstate $|\Psi_{LM\alpha}\rangle$ has electron pairs with coupled angular momentum L_{12} is given in terms of the coefficients of fractional parentage by

$$P_{L\alpha}(L_{12}) = \sum_{L',\alpha'} |G_{L\alpha,L'\alpha'}(L_{12})|^2 \tag{3.15}$$

Naturally, the sum of all pair probabilities over all possible values the pair angular momentum L_{12} is necessarily equal to 1:

$$\sum_{L_{12}} P_{L\alpha}(L_{12}) = 1. \tag{3.16}$$

The coefficients of fractional grandparentage of a given wavefunction, and the corresponding pair probabilities, can be calculated directly using angular momentum theory, but it is perhaps simpler to extract the pair probabilities from the tensor set by projecting them out of the n-body wavefunctions. We begin with the following expression, the partial inner product of a two-body tensorial set on an n-body tensorial set:

$$(l^2 L_{12}|l^n;\alpha L\rangle = \sum_{L'\alpha'} G_{L\alpha,L'\alpha'}(L_{12})(3\ldots n]\}l^{n-2}\alpha' L'\} \tag{3.17}$$

We have dropped the notation of Fano and Racah on the left side of the expression in order to simplify the expressions- the absence of the M indices should be sufficient to indicate that these are tensorial sets rather than the elements of tensorial sets. We have used curved braces for the pair tensorial set on the left instead of an angle bracket because the expression is not a full inner product, but is itself a set of $n-2$ particle functions. The pair probabilities (and consequently, the coefficients of fractional parentage) can be calculated using the following constructed expression:

$$\langle l^n;\alpha L|l^2 L_{12})(l^2 L_{12}|l^n;\alpha L\rangle = \sum_{L'\alpha'} |G_{L\alpha,L'\alpha'}(L_{12})|^2 = P(L_{12}) \tag{3.18}$$

Note that the pair probability is evaluated by using a projection operator, $\mathcal{P}_{L_{12}} = |l^2 L_{12})(l^2 L_{12}|$. The pair probabilites of (3.18) can be calculated more directly in terms of the elements of the irreducible set by summing over the elements of the two-particle irreducible set,

$$P_{L\alpha}(L_{12}) = \sum_{M_{12}} \langle l^n; \alpha LM | l^2 L_{12} M_{12})(l^2 L_{12} M_{12} | l^n; \alpha LM \rangle \tag{3.19}$$

In order to evaluate equation (3.19), we will use Slater determinants to perform the projection of the two-body state onto the n-body state:

$$(l^2; L_{12} M_{12} | l^n L M \alpha \rangle = (\Psi_{L_{12}}(1,2) | \Psi_{LM\alpha}(1,2,\ldots,n)\rangle \tag{3.20}$$

Here $|\Psi_{L_{12}M_{12}}(1,2)\rangle \equiv |l^2; L_{12}M_{12}\rangle$ is an antisymmetric angular momentum pair state for the electrons labeled 1 and 2, and $|\Psi_{LM\alpha}(1,2,\ldots,n)\rangle \equiv |l^n; LM\alpha\rangle$ is an antisymmetric angular momentum eigenstate of all n electrons. We can write the wavefunctions of these two states in coordinate space as the sum over the Slater determinants constructed from the same single-particle basis,

$$\begin{aligned} \Psi_{L_{12}M_{12}}(x_1, x_2) &= \sum_j a_j(L_{12}M_{12}) \Phi_j(x_1, x_2) \\ \Psi_{LM\alpha}(x_1, x_2, \ldots x_n) &= \sum_k a_k(LM\alpha) \Phi_k(x_1, x_2, \ldots, x_n). \end{aligned} \tag{3.21}$$

As in section 3.1, x_i is a shorthand for of all the coordinates (and spin, if included) of the i^{th} electron. The projection of the two-particle wavefunction onto the n-particle wavefunction is given in terms of the two- and n-body Slater determinants by

$$\Psi'(x_3, \ldots, x_n) = \sum_j \sum_k a_j^*(L_{12}M_{12}) a_k(LM\alpha) \int \Phi_j^*(x_1, x_2) \Phi_k(x_1, x_2, \ldots x_n) dx_1 dx_2. \tag{3.22}$$

The integral of 3.22 can be evaluated directly without explicit integration by using the orthonormality of the single particle wavefunctions to develop the following theorem.

Theorem 3.1. *Given a two particle Slater determinant,*

$$\Phi_j(x_1, x_2) = \frac{1}{\sqrt{2}} \begin{vmatrix} \phi_1(x_1) & \phi_1(x_2) \\ \phi_2(x_1) & \phi_2(x_2) \end{vmatrix} = \frac{1}{\sqrt{2}} \left[\phi_1(x_1)\phi_2(x_2) - \phi_1(x_2)\phi_2(x_1)\right] \tag{3.23}$$

constructed from the set of two single-particle wavefunctions, $\mathcal{S}_j = \{\phi_1, \phi_2\}$*, and an n-particle Slater determinant*

$$\Phi_k(x_1, \ldots x_n) = \frac{1}{\sqrt{n!}} \begin{vmatrix} \phi'_1(x_1) & \phi'_1(x_2) & \cdots & \phi'_1(x_n) \\ \vdots & \vdots & & \vdots \\ \phi'_n(x_1) & \phi'_n(x_2) & \cdots & \phi'_n(x_n) \end{vmatrix}, \tag{3.24}$$

constructed from the set of n single-particle wavefunctions, $\mathcal{S}_k = \{\phi'_1, \phi'_2, \ldots, \phi'_n\}$*, where* $\mathcal{S}_j$ *and* $\mathcal{S}_k$ *are subsets of the same overset of orthonormal, single-particle wavefunctions with a consistently defined ordering, then the integral over the coordinates* x_1 *and* x_2 *of the inner product of the two Slater determinants,*

$$F(x_3, x_4, \ldots, x_n) = \int \Phi^*_j(x_1, x_2)\Phi_k(x_1, x_2, \ldots x_n)dx_1dx_2, \tag{3.25}$$

is zero unless ϕ_1 *and* ϕ_2 *from* $\mathcal{S}_j$ *are also elements of* $\mathcal{S}_k$*. If* $\phi'_i = \phi_1$ *and* $\phi'_j = \phi_2$ *for some* ϕ'_i *and* ϕ'_j *in* $\mathcal{S}_k$*, then the integral is itself a Slater determinant of* $(n-2)$ *particles formed from* $\mathcal{S}_{k-j} = \mathcal{S}_k \setminus \mathcal{S}_j$*, (the set of single particle wavefunctions of* Φ_k *minus* $\phi'_i = \phi_1$ *and* $\phi'_j = \phi_2$*) times a constant,*

$$F(x_3, \ldots x_n) = (-1)^{i+j+1} \sqrt{\frac{2}{n(n-1)}} \Phi^{(j)}_{red,k}(x_3, \ldots, x_n). \tag{3.26}$$

The Slater determinant in (3.26)*,*

$$\Phi^{(j)}_{red,k}(x_3,\ldots,x_n) = \frac{1}{\sqrt{(n-2)!}} \begin{vmatrix} \phi'_1(x_3) & \cdots & \phi'_1(x_n) \\ \vdots & & \vdots \\ \phi'_n(x_3) & \cdots & \phi'_n(x_n) \end{vmatrix}, \tag{3.27}$$

will be called the Slater determinant of j reduced by k. The indices i and j arise out of the arbitrary ordering of the single-particle wavefunctions necessary for the construction of the Slater determiants.

Proof. If ϕ_1 and ϕ_2 are not both elements of $\mathcal{S}_k$, it follows trivially from the orthogonality of the single particle wavefunctions comprising the Slater determinants that the integral in (3.25) must equal 0. Assume, for example, that ϕ_1 is absent from $\mathcal{S}_k$. Then by (3.24), the definition of Φ_k, particle 1 (or paritcle 2) does not occupy ϕ_1 in any terms of Ψ_k. We expand then the Slater determinant about the column for particle 1, for example,

$$\Phi_k(x_1,\ldots x_n) = \frac{1}{\sqrt{n!}}\left[\phi'_1(x_1)f_1(x_2,\ldots,x_n) + \phi'_2(x_1)f_2(x_2,\ldots,x_n) + \right. \\ \left. \ldots + \phi'_n(x_1)f_n(x_2,\ldots,x_n)\right], \tag{3.28}$$

where the $(n-1)$ functions f_a are all determinants times ± 1. It is clear that, since ϕ_1 is not found among the ϕ'_i, then the integral over particle 1 is zero for all terms in the sum. This result obviously also holds for ϕ_2.

And so, the integral is non-zero only if ϕ_1 and ϕ_2 are also both elements of $\mathcal{S}_k$. Now, let us assume that $\mathcal{S}_k$ contains the following two wavefunctions $\phi_i = \phi_1$ and $\phi_j = \phi_2$. The integral of (3.25) can be carried out by using the Laplace expansion of the Slater determinants about the first two columns of (3.24). The majority of the terms in the expansion will be zero due to the orthogonality of the single particle

functions; the remaining non-zero part of (3.25) is

$$F(x_3,\dots x_n) = \frac{1}{\sqrt{2\times n!}}\begin{vmatrix} \phi'_1(x_3) & \cdots & \phi'_1(x_n) \\ \vdots & & \vdots \\ \phi'_n(x_3) & \cdots & \phi'_n(x_n) \end{vmatrix}$$
$$\times \int \left[(-1)^{i+j+1}\phi^*_1(x_1)\phi^*_2(x_2)\phi'_i(x_1)\phi'_j(x_2) - (-1)^{i+j}\phi^*_2(x_1)\phi^*_1(x_2)\phi'_j(x_1)\phi'_i(x_2)\right] dx_1dx_2 \tag{3.29}$$

The determinant of (3.29) is itself an unnormalized $(n-2)$ particle Slater determinant of particles $3,4,\dots,n$ formed from the set $\mathcal{S}_{k-j} = \mathcal{S}_k \setminus \mathcal{S}_j$, (the set of single particle wavefunctions of Φ_k minus $\phi'_i = \phi_1$ and $\phi'_j = \phi_2$).

Integrating (3.28) and incorporating the definition of the reduced Slater determinant defined in (3.27) yields the result

$$\int \Phi^*_j(x_1,x_2)\Phi_k(x_1,x_2,\dots x_n)dx_1dx_2 = (-1)^{i+j+1}\sqrt{\frac{2}{n(n-1)}}\Phi^{(j)}_{red,k}(x_3,\dots,x_n). \tag{3.30}$$

□

Returning to (3.22), the projection of the two-particle wavefunction onto the n-particle wavefunction reduces to

$$\Psi'(x_3,\dots,x_n) = \sqrt{\frac{2}{n(n-1)}}\sum_j\sum_k (-1)^{i+j+1}a^*_j(L_{12}M_{12})a_k(LM\alpha)\Phi^{(j)}_{red,k}(x_3,\dots,x_n). \tag{3.31}$$

And as a result, the inner product $\langle l^n; L\alpha | l^2; L_{12})(l^2; L_{12} | l^n; L\alpha\rangle$ is given by

$$\begin{aligned} P_{L\alpha}(L_{12}) &= \sum_{M_{12}} \langle l^n; LM\alpha | l^2; L_{12}M_{12})(l^2; L_{12}M_{12} | l^n; LM\alpha\rangle \\ &= \frac{2}{n(n-1)} \sum_{\substack{j,j',\\ k,k'}} \Bigg[(-1)^{j+j'+k+k'} a^*_{k'}(LM\alpha) a_{j'}(L_{12}M_{12}) a_k(LM\alpha) a^*_j(L_{12}M_{12}) \\ &\qquad \times \int \Phi^{(j')}_{red,k'}(x_3, \ldots, x_n) \Phi^{(j)}_{red,k}(x_3, \ldots, x_n) dx_3 \ldots dx_n \Bigg] \end{aligned} \tag{3.32}$$

Note that the integral in equation (3.32) is not a simple delta function in k and k' or in j and j'. Instead, the integral is equal to 1 when the sets that define the reduced Slater determinants, $\Phi^{(j)}_{red,k}$ and $\Phi^{(j')}_{red,k'}$ are equal. That is, the integral is 1 if and only if $\mathcal{S}_{k-j} \equiv \mathcal{S}_k \setminus \mathcal{S}_j$ is exactly equal to $\mathcal{S}_{k'-j'} = \mathcal{S}_{k'} \setminus \mathcal{S}_{j'}$.

Using the result given in equation (3.32), the pair probabilities in an 8 electron system for the Laughlin incompressible ground state at filling factor of $\nu = 1/3$ and for the Jain incompressible ground state at $\nu = 2/5$ are presented in figure 3.4. The pair probabilities are presented as a function of the relative pair angular momentum $R = 2l - L_{12}$. Since both of these filling factors correspond to the lowest Landau level, $l = l_0 = Q$.

As can be seen in figure 3.4, electrons in the $L = 0$ ground states for both the $\nu = 1/3$ and the $\nu = 2/5$ states strongly avoid pair states with $R = 1$. Electron pairs in both ground states avoid the $R = 1$ highest pair angular momentum as a result of the strong repulsion of the pair angular momentum in the lowest Landau level. States in which electron pairs dramatically avoid high angular momentum states are said to be Laughlin correlated, and the avoidance of such high angular momentum pair states is known as Laughlin-Jastrow correlations.

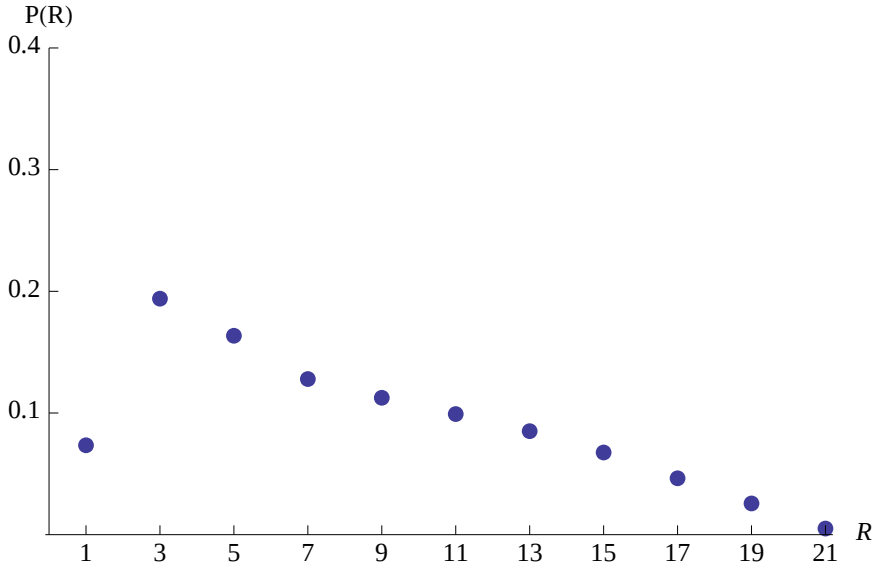

(a) Pair probabilities for the ground state at $\nu = 1/3$ filling.

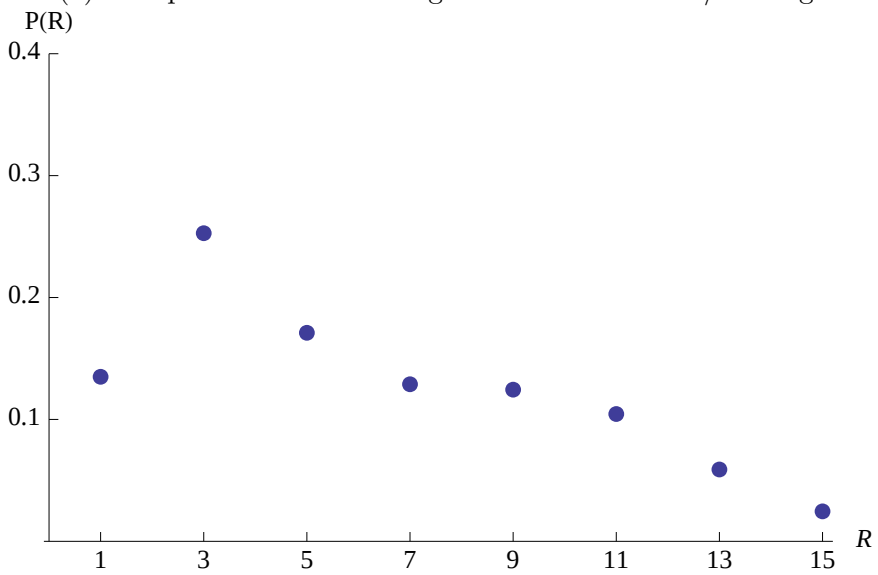

(b) Pair probabilities for the ground state at $\nu = 2/5$ filling.

Figure 3.4: The pair probabilites for the $L = 0$ ground states for 8 electrons as a function of the relative pair angular momentum, $R = 2l - L_{12}$, where $l = Q$ because the electrons are in the lowest Landau level. Subfigure (a) corresponds to the $L = 0$ ground state shown in figure 3.1; subfigure (b) shows the pair probabilities for the $L = 0$ ground state of figure 3.3. Notice that, for both ground states, the pair probability for $R = 1$ is significantly depressed: in other words, electron pairs in both ground states strongly avoid pair states with very large pair angular momentum. This avoidance of pair states with $R = 1$ is known as Laughlin correlations or Laughlin-Jastrow correlations.

Chapter 4

Landau level mixing

Up until this point, we have used the single Landau level approximation in order to calculate the electron correlations in the quantum Hall system. This approximation assumes that the magnetic field, B, is sufficiently strong that electrons cannot transition to other Landau levels, which restricts the single-particle Hilbert space to that of a single, isolated Landau level. It also assumes that electrons in a closed Landau level do not contribute to the behavior of electrons in other shells.

This single Landau level approximation is most valid in the regime of extremely strong magnetic fields, where the ratio γ of the cyclotron energy $\hbar\omega_c$ to the Coulomb energy $V_c = e^2/4\pi\epsilon\lambda$, where $\lambda = \sqrt{\hbar/Be}$ is the magnetic length, is very large. In this case, the Coulomb energy is the only relevant energy scale, and the Coulomb interaction alone controls the electron correlations. However, in typical quantum Hall experiments, the ratio γ is not dramatically greater than 1, and inter-Landau level electronic excitations should be taken into account. For example, assuming the experiment is being performed on very cold gallium arsenide, γ is approximately 1.26 for a moderately strong magnetic field of 10 Tesla. The physical constants for GaAs at 4 Kelvin have been taken from [Haynes (2012)]. The contribution of multiple Landau levels to the behavior of electrons largely, but not completely, confined to a single Landau level is known as Landau level mixing.

In theory, Landau level mixing could be examined directly using the same techniques of exact numerical diagonalization presented in Chapter 3 for many-electron systems. Unfortunately, numerical diagonalizations for many-particle systems in the Hilbert space including multiple Landau levels are prohibitively large to be carried out for all but a very small number of particles [Wójs and Quinn (2006); Yoshioka (1984)]. There have been a few other attempts to treat Landau level mixing. A recent paper [Bishara and Nayak (2009)] treated the effects of LL mixing on the pair pseudopotentials by perturbation theory to second order in $\kappa = \gamma^{-1}$. Earlier works evaluated LL mixing through numerical diagonalization of systems with few particles [Wójs and Quinn (2006); Yoshioka (1984)], or by the random phase approximation [Morf et al. (2002)].

In this chapter, we will incorporate Landau level mixing into the pseudopotential $V(L)$ by numerically diagonalizing the Hamiltonian within Hilbert subspaces restricted by the total angular momentum, L and the non-interacting energy of the states. Each Hilbert subspace will include all excited states of the same angular momentum with non-interacting energies within $x\hbar\omega_c+\delta$ of an initial pair state. Here, x is an integer representing the number of excitations and δ is a minor correction factor to the energy arising from the spherical geometry that becomes vanishingly small on a large sphere. In the calculations for LL1, we explicitly include states with quasiparticles created from the filled LL0 shell. I will evaluate the Landau level mixing pseudopotentials in the lowest and first excited Landau levels (LL0 and LL1, respectively) in the short range (large L), since the short range pseudopotentials have the largest effect on electron correlations.

4.1 Level mixing in the lowest Landau level

It is relatively simple to examine how Landau level mixing affects the pseudopotential of the lowest Landau level (LL0). The Hamiltonian of the system is, again, a sum

over the single-particle energies plus the Coulomb interaction,

$$\hat{H} = \frac{e^2}{4\pi\epsilon\lambda_0}\left[\gamma\sum_{i=1}\frac{(\mathbf{l_i}-\hbar Q\hat{R}_i)^2}{2Q\hbar^2}+\sum_{i<j}\frac{\lambda_0}{r_{ij}}\right], \tag{4.1}$$

where Q is the magnetic monopole strength with $2Q =$ an integer, and $l_n = Q + n$ is the shell angular momentum of an electron in LLn.

We begin with a pair of electrons both in LL0 in an angular momentum eigenstate, $|l_0^2; L\rangle$ with total angular momentum L and a non-interacting magnetic energy $\hbar\omega_c$. As can be seen in section 2.5, the spatial symmetry of the angular momentum eigenstate is determined by the spin symmetry of the electron pairs: given that $R = 2l_0 - L$ for electrons in LL0, spin triplet electrons are restricted to odd values of R, while spin singlet electrons take only even values of R. As a result of the Wigner-Eckart theorem, each of these initial ground states, $|l_0^2; L\rangle$, interacts only with states that have the same total angular momentum, L. As such, numerical diagonalizations will be performed on basis sets of total angular momentum pair states with the same angular momentum and same spin.

For each L, the LL0 pair state $|l_0^2; L\rangle$ will be the initial ground state used to construct the basis set for numerical diagonalization. The remainder of each L-basis set consists of all magnetically excited pair states within $x\hbar\omega_c$ with the same total angular momentum as the initial ground state. The matrix to be diagonalized is not large for small values of x. For example, if including up to $x = 2$ excitations, the basis set for a single value of the total angular momentum L contains only 4 basis states: $|l_0^2; L\rangle$ with magnetic energy $\hbar\omega_c$, $|l_0, l_1; L\rangle$ with magnetic energy $2\hbar\omega_c$, and $|l_0, l_2; L\rangle$ and $|l_1^2; L\rangle$, both with magnetic energy $3\hbar\omega_c$.

The lowest eigenenergy of the numerical diagonalization for each L is one term, $V(L)$, of the pseudopotential including Landau level mixing. The numerical diagonalizations for $R = 2l_0 - L = 0, 1, \ldots 5$ were performed for a wide range of magnetic fields between 2 and 120 Tesla for magnetic monopole strengths $Q = 5, 10, \ldots, 50$. For each magnetic field, a functional fit was performed in powers of

Q^{-1} up to Q^{-2}. Taking the limit as Q approaches ∞ of the functional fit gives a good approximation to the expected pseudopotential on an infinite sphere, which corresponds to an infinite plane. The Landau level mixing pseudopotentials including up to 4 excitations are presented as function of $\kappa(B) = 1/\gamma(B) \propto \sqrt{B}$ in Fig. (4.1).

As can be seen in Fig. (4.1), the Landau level mixing pseudopotentials in the lowest Landau level vary nearly linearly in $\kappa(B) = \gamma^{-1}(B)$. For all but the highest angular momentum state, $R = 0$, the effect of Landau level mixing is only on the order of $\approx 1\%$ for even relatively weak magnetic fields (≈ 2T). It is only the $R = 0$ term of the pseudopotential that is noticeably changed by the inclusion of Landau level mixing: in this case, the effect is on the order of at most $\approx 10\%$. In addition, because the $R = 0$ term is the only term that is even moderately affected by Landau level mixing, we predict that Landau level mixing contributes very little to electrons in the lowest Landau level. This result agrees with an earlier numerical calculation, which determined that the effect of Landau level mixing on the $\nu = 1/3$ state is minimal [Yoshioka (1984)].

Note that, in the presence of a strong magnetic field, the electron spins will most likely align with the magnetic field. As such, they will be in the spin-aligned triplet state and will be unable to form coupled states with even relative angular momentum, R. As a result, the relatively stronger effect of Landau level mixing on the $R = 0$ pseudopotential should be entirely invisible in systems that are totally spin polarized.

4.2 Level mixing in the first excited Landau level

To determine the effect of Landau level mixing on the first excited Landau level we begin with an initial ground state with a pair of electrons in the first excited Landau level and construct a basis set that includes magnetically excited states within $x\hbar\omega_c$ of this initial state. As in the Landau level 0 mixing calculations, we can use the Wigner-Eckart theorem to separate diagonalizations of different total angular momenta, L

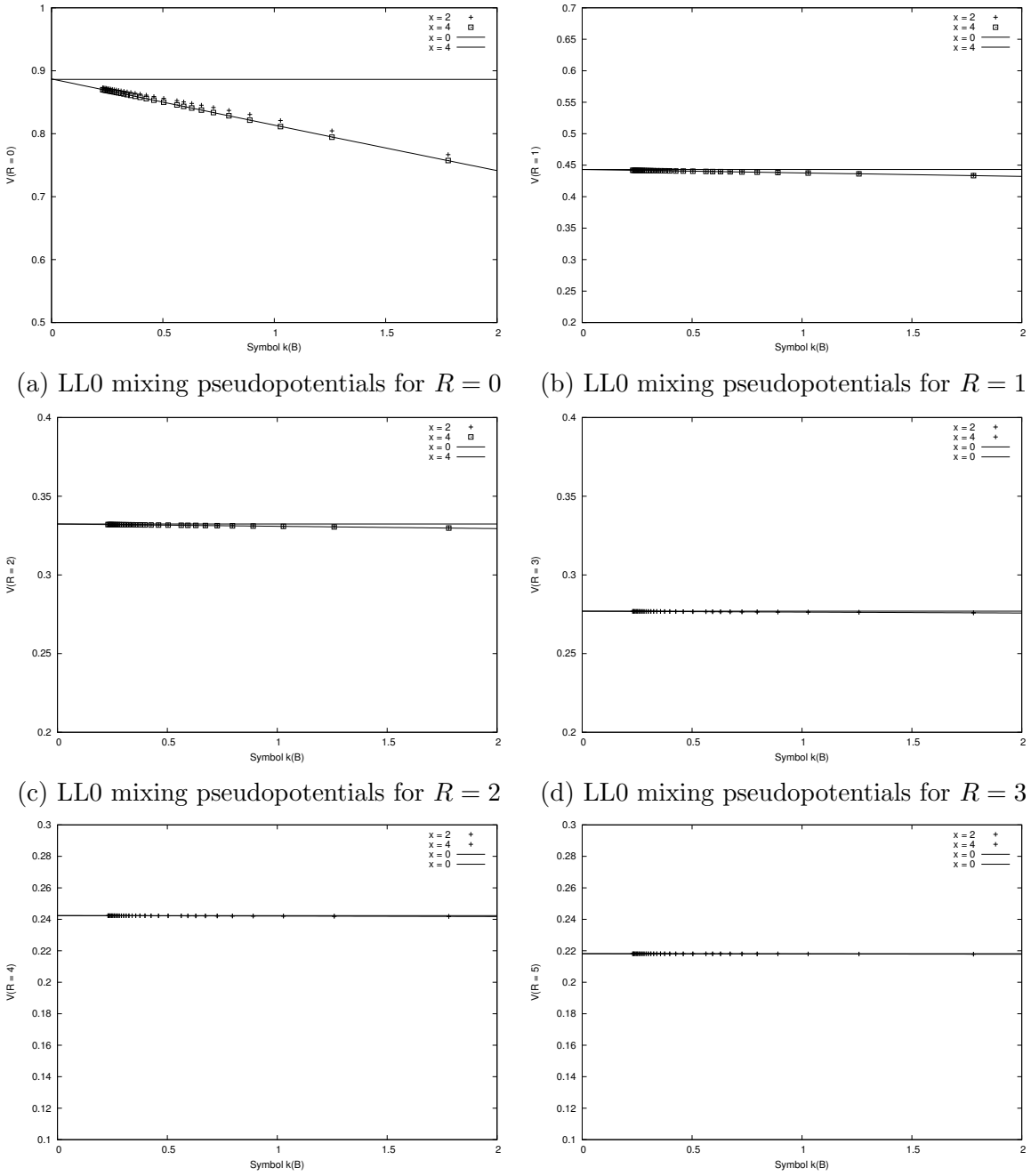

(a) LL0 mixing pseudopotentials for $R = 0$ (b) LL0 mixing pseudopotentials for $R = 1$

(c) LL0 mixing pseudopotentials for $R = 2$ (d) LL0 mixing pseudopotentials for $R = 3$

(e) LL0 mixing pseudopotentials for $R = 4$ (f) LL0 mixing pseudopotentials for $R = 5$

Figure 4.1: The pseudopotentials for pairs in LL0 as modified by LL mixing for $R = 0, 1, \ldots, 5$ are presented as a function of $\kappa(B) = e^2/\hbar\omega_c 4\pi\epsilon\lambda$, $\kappa \propto B^{-1/2}$, where B is the magnetic field strength. The $x = 2$ and 4 excitation curves are the results for including all states within an energy cutoff of $x\hbar\omega_c$ of the initial LL0 pair state in the Hilbert space.The horizontal line in each plot is the non-mixing pseudopotential. The pseudopotentials are given in units of the Coulomb energy.

However, unlike in the lowest Landau level, LL0, this initial state must also include the totally filled Landau level 0 shell, which contains $2Q + 1$ spin down and $2Q + 1$ spin up electrons. The filled LL0 spin shells can equivalently be considered a vacuum ground state from which electron-hole pairs can be created. So, the numerical diagonalization must include not only magnetic excitations of the LL1 electrons, but also the creation of electron-hole quasiparticles. Because it is considerably more numerically challenging to include both spin up and spin down, as a first approximation, we consider a system that entirely ignores electron with spins that are not aligned with the magnetic field. So, in this model, we define the initial ground states as the eigenvectors of total angular momentum L with a pair of spin up electrons in LL1 and a totally filled spin up LL0 shell. These ground states can be written as $|l^2_{1\uparrow}; L\rangle$, where the filled LL0 spin up shell is implicitly included as a vacuum state, and the filled LL0 spin down shell is treated as a closed and inactive bystander.

The remainder of each total L basis set is constructed from its initial eigenvector ground state $|l^2_{1\uparrow}; L\rangle$ by including all possible magnetically excited states with the same total angular momentum. For example, one singly excited state (with magnetic energy within $\approx \hbar\omega_c$ of the initial ground state) is the state written $|l_{1\uparrow}, l_{2\uparrow}; L\rangle$. However, with the same number of magnetic excitations are the set of all states with 3 electrons in LL1 and a single hole in LL0. These states can be written as $|l^3_{1\uparrow}, h_{0\uparrow}; L\alpha\rangle$, where $h_{0\uparrow}$ represents an electron hole created in the Landau level 0 spin up shell, and α is an additional label to distinguish similar orthogonal states with the same total L. Because the Hamiltonian lacks any spin operators, the only excited states included in the Hilbert subspace are those that share the same total z-component of spin, S_z. In other words, when constructing the excited states, no spin flips are considered for the model.

For each allowed angular momentum L, we diagonalize the Hamiltonian to get the lowest energies. The lowest energy eigenvalues are the pair energies, $E^x_2(L, B)$, which are a function of the angular momentum L, and the magnetic field. However,

the two body energies calculated by numerical diagonalization, $E_2^x(L,B)$, are not the pseudopotentials as they were in the LL0 diagonalizations. Instead, the energy eigenvalues given by this procedure also include the quasiparticle and the vacuum energies, which also depend on Landau level mixing and must be subtracted from the pair energies to give the pseudopotential.

Fortunately, the quasiparticle energy and the vacuum energy as affected by Landau level mixing can also be found through the same procedure as the two-electron energies. To evaluate the energy of a single quasiparticle including up to x magnetic excitations, we define a single initial ground state, $|l_{1\uparrow}; L\rangle$. The initial ground state implicitly includes a totally filled LL0 ground state, and its total angular momentum L is necessarily equal to the shell angular momentum, l_1 of LL1. The single initial ground state connects only to magnetically excited states of the same total angular momentum, e.g. $|l_{1\uparrow}^2, h_{0\uparrow}; L\rangle$, where here $L = l_1$.

The single-electron ground state and all magnetically excited states with angular momentum $L = l_1$ form the basis set for diagonalizing the Hamiltonian. Upon diagonalization, the resulting lowest energy including up to x magnetic excitations is the single-particle mixing energy, $E_1^x(B)$ and is function of the magnetic field. This energy in turn also includes the energy of the vacuum state, $E_0^x(B)$ which must also be calculated in the same manner.

The initial ground state for the vacuum energy calculation is the state with no LL1 electrons, and a totally filled lowest Landau level shell. The total angular momentum of this state is $L = 0$, and again by the Wigner-Eckart theorem, it connects only to magnetically excited states with the same angular momentum. Constructing the basis set restricted by the same energy cutoff, x, using the same procedure and diagonalizing gives the lowest energy eigenvalue, $E_0^x(B)$, which is the vacuum energy.

The pseudopotential, $V^x(L,B)$, for a finite number, x, of allowed magnetic excitations is given by subtracting the energy of two quasiparticles from the pair energy given by direct numerical diagonalization, $E_2^x(L,B)$. Because twice the quasiparticle energy includes the vacuum energy twice, it is necessary to add the

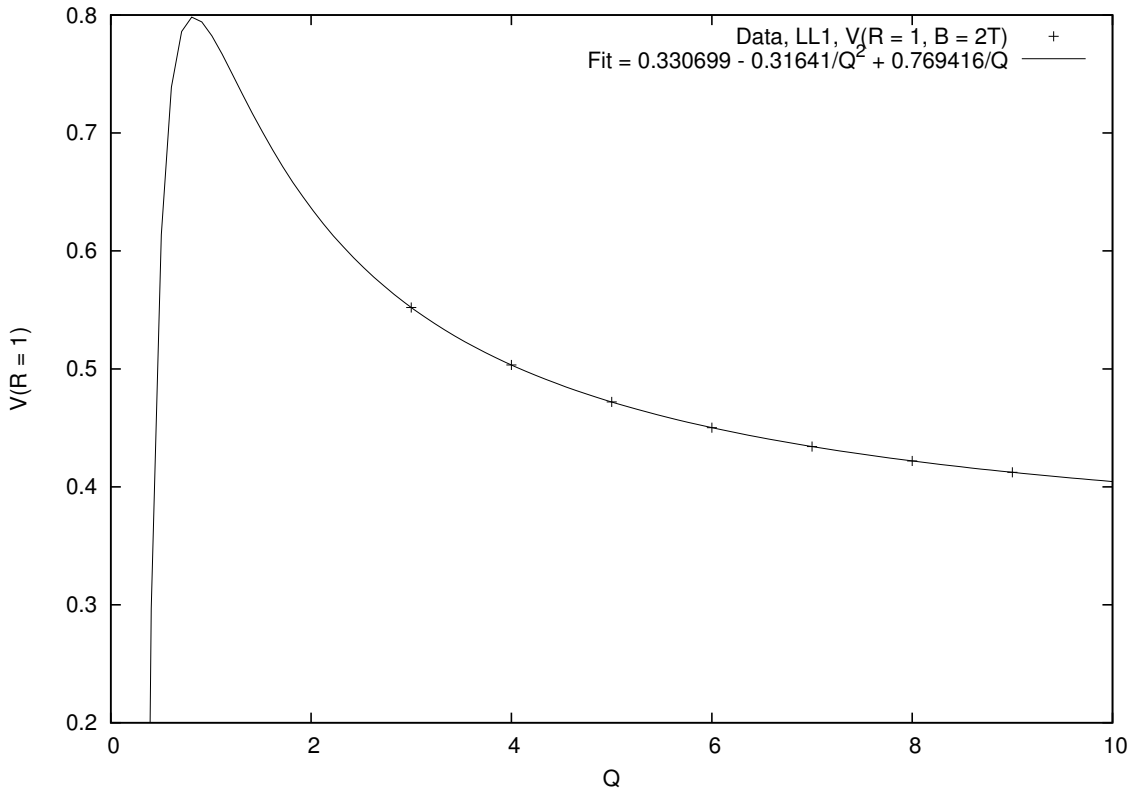

Figure 4.2: The LL1 mixing pseudopotential for $R = 2l_1 - L = 1$ and a magnetic field of B = 2, including all states within $2\hbar\omega_c$ of the initial LL1 pair states, as a function of the monopole strength, Q. This plot is an example of the extrapolations in powers of Q^{-1}. For this model, electrons with spins anti-aligned with the magnetic field (spin down) have been treated as non-participatory. The pseudopotential is given in units of the Coulomb energy.

vacuum energy back in to get the pseudopotential.

$$V^x(L, B) = E_2^x(L, B) - 2E_1^x(B) + E_0^x(B) \tag{4.2}$$

The results for the pseudopotential ignoring the spin down LL0 shell were carried out with $Q = 3, \ldots, 30$ for $x = 1$ and $Q = 3, \ldots, 9$ for $x = 2$ for a wide range of magnetic fields. For each magnetic field a numerical best fit for the data was found for the function $f(Q) = a + bQ^{-1} + cQ^{-2}$. A sample data data set and functional fit is shown in Figure 4.2.The value of this fit function in the limit as Q becomes

infinite for each value of the magnetic field was recorded and plotted as a function of $\kappa(B) = 1/\gamma(B) \propto \sqrt{B}$ in the left column of Figure 4.3.

The model above can be improved by including excitations from the LL0 spin down shell. The interaction Hamiltonian remains the same, and as such, electrons are not allowed to flip spins in the model. As a result, although the newly included spin down electrons and holes interact with the spin up electrons and holes, there will be no exchange contribution for two-body matrix elements between spin up and spin down particles. The mixing pseudopotentials for a spin parallel pair of electrons in LL1 including opposite spin excitaitons were calculated using the same procedure as before, and are presented in the right column of Figure 4.3. Including many more excited states unfortunately increases the numerical size of the problem significantly, such that diagonalizations were carried out for $Q = 2, \ldots, 15$ for $x = 1$ and for only $Q = 2, \ldots, 5$ for $x = 2$. With so few points, the extrapolations in powers of $1/Q$ are not definitive, but are not qualitatively different from the results of the smaller system ignoring spins.

As a final model, we also performed the same procedure again, but this time for an electron pair in LL1 with antiparallel spins. This model necessarily included excitations of both spin up and spin down LL0 electrons, and included states constructed from the initial angular momentum ground states, $|l_{1\uparrow}, l_{1,\downarrow}; L\rangle$. In this case, it was too numerically challenging to evaluate the mixing pseudopotentials including two magnetic excitations, $x = 2$, but the $x = 1$ results are presented in Figure 4.4.

A primary difference between the first model and the remaining two is the largest Q for which numerical diagonalization could be performed. For the same value of Q, the system including both LL0 spin excitations is always significantly larger than the systems that ignore excitations from the LL0 spin down shell. As a result, the extrapolations in powers of Q^{-1} are most accurate for the first model because it was computationally possible to diagonalize more and larger systems for $x = 2$. For this reason, and because the two-excitation results are qualitatively similar for all three

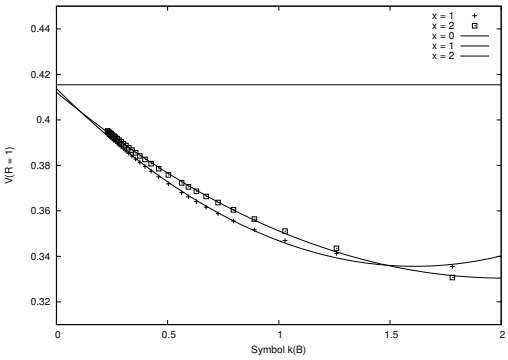

(a) V(R = 1) versus $\kappa(B)$, ignoring spin down LL0 excitations.

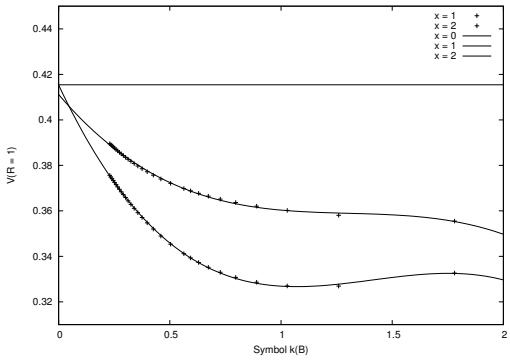

(b) V(R = 1) versus $\kappa(B)$, including spin down LL0 excitations.

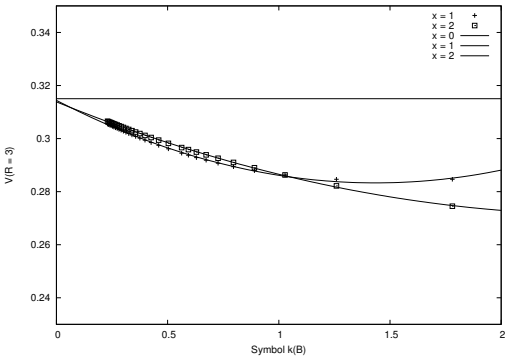

(c) V(R = 3) versus $\kappa(B)$, ignoring spin down LL0 excitations.

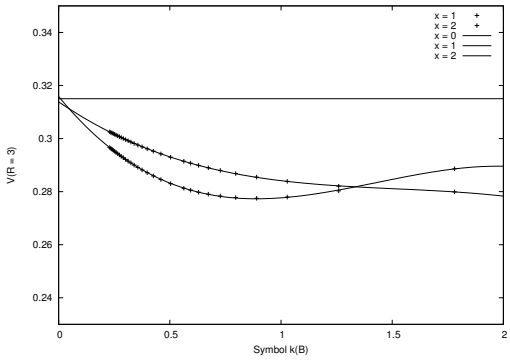

(d) V(R = 3) versus $\kappa(B)$, including spin down LL0 excitations.

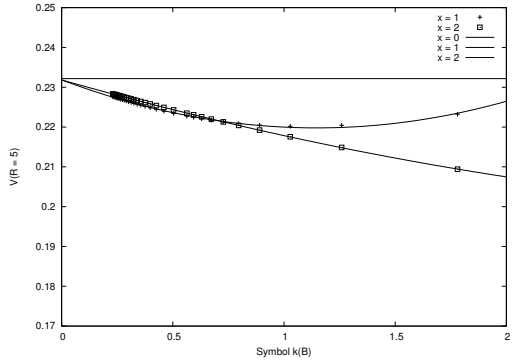

(e) V(R = 5) versus $\kappa(B)$, ignoring spin down LL0 excitaitons.

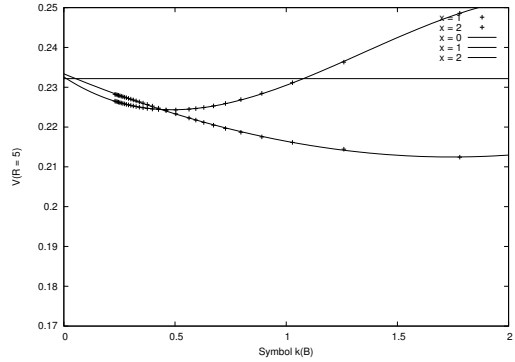

(f) V(R = 5) versus $\kappa(B)$, including spin down LL0 excitations.

Figure 4.3: The pseudopotentials in LL1 as modified by LL mixing for $R = 1, 3, 5, 7$ are presented as a function of $\kappa(B) = e^2/\hbar\omega_c 4\pi\epsilon\lambda$, $\kappa \propto B^{-1/2}$, where B is the magnetic field strength. The $x = 1$ and 2 excitation curves are the results for including all states within an energy cutoff of $x\hbar\omega_c$ of initial LL1 pair states in the Hilbert space. Excited states include particle-hole excitations from the lowest Landau level. In this model, the initial electron pair in LL1 are assumed to both be in a spin down state, and we completely ignore the LL0 spin up electrons. The horizontal line in each plot is the non-mixing pseudopotential. The pseudopotentials are given in units of the Coulomb energy.

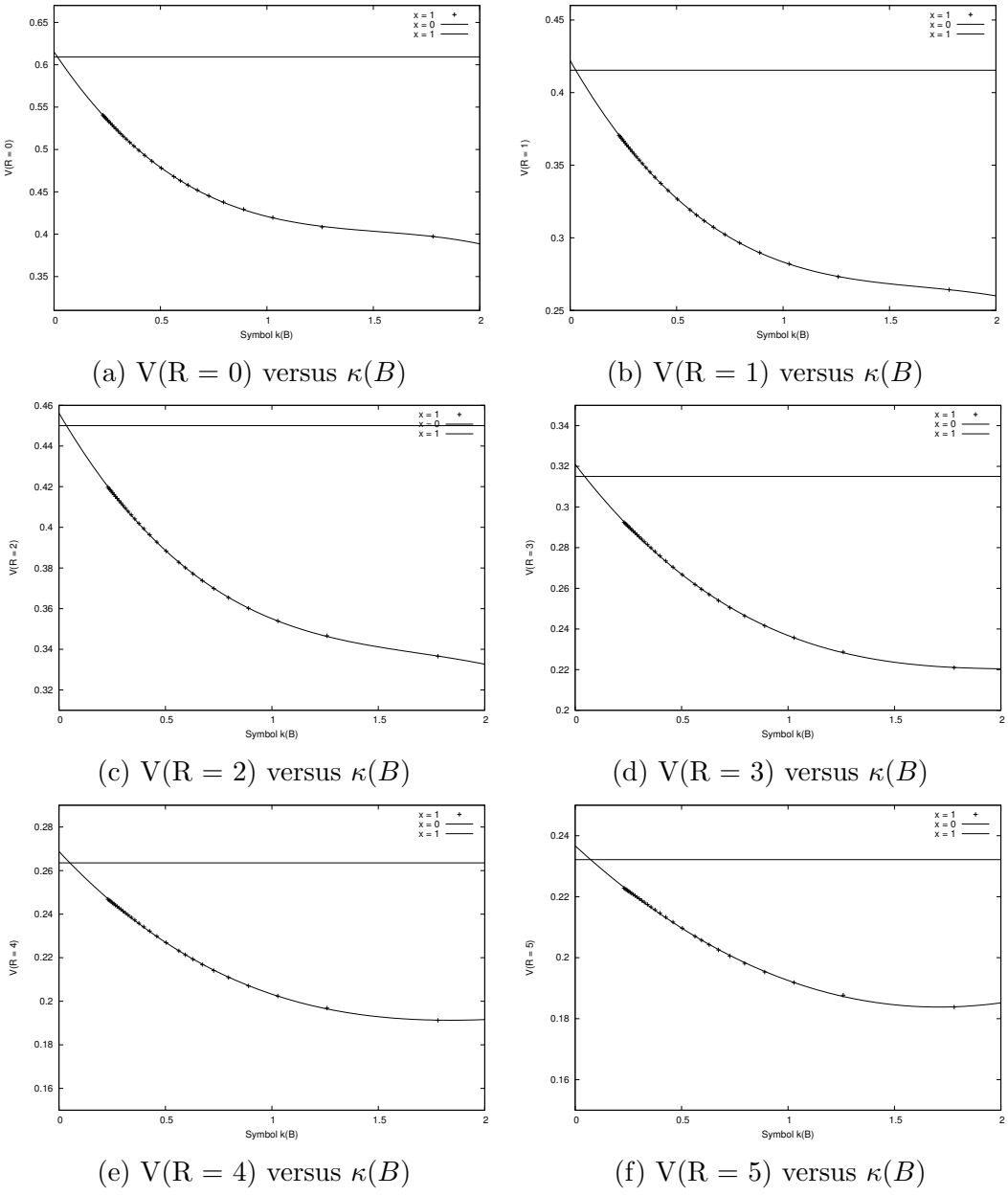

(a) V(R = 0) versus $\kappa(B)$ (b) V(R = 1) versus $\kappa(B)$

(c) V(R = 2) versus $\kappa(B)$ (d) V(R = 3) versus $\kappa(B)$

(e) V(R = 4) versus $\kappa(B)$ (f) V(R = 5) versus $\kappa(B)$

Figure 4.4: The pseudopotentials in LL1 as modified by LL mixing for $R = 0, \ldots, 5$ are presented as a function of $\kappa(B) = e^2/\hbar\omega_c 4\pi\epsilon\lambda$, $\kappa \propto B^{-1/2}$, where B is the magnetic field strength. The $x = 1$ excitation curves are the results for including all states within an energy cutoff of $x\hbar\omega_c$ of initial LL1 pair states in the Hilbert space. Excited states include particle-hole excitations from the lowest Landau level. In this model, the initial state has one electron of spin up and one of spin down in LL1, and both LL0 spins are included. The horizontal line in each plot is the non-mixing pseudopotential. The pseudopotentials are given in units of the Coulomb energy.

systems, the remaining discussion will focus on the results in the system ignoring spin down excitations from LL0.

In stark contrast to the lowest Landau level, the first excited Landau level appears to be somewhat strongly affected by Landau level mixing. The effect of mixing for moderate magnetic fields is to depress the pair pseudopotentials. For example, in the case where we have ignored electronic excitations from the LL0 spin down shell, the effect of Landau level mixing is to reduce the pair pseudopotentials by a factor on the order to 10-20% for magnetic fields in the range of ≈ 10 tesla for the highest pair angular momenta, $R = 1$.

The pair pseudopotential reduction is strongest for the largest pair angular momentum, $R = 1$, indicating that Landau level mixing in LL1 acts to reduce the repulsion for tightly bound electrons. For larger values of R, or pair states with lower total angular momentum, the Landau level mixing reduction to the pseudopotential $V(R)$ becomes decreasingly strong. For example, at a magnetic field of 10 Tesla in the system, the LL mixing decreases $V(R = 1)$ by a little over 15% when two excitations are included. The percent reduction in the pseudopotential decreases as R increases swiftly, such that the pseudopotential including LL mixing at $R = 7$ is only 3% smaller than the non-mixing pseudopotential. The relatively stronger decrease in the small R pseudopotentials suggests that Landau level mixing in the first excited Landau level increases the probability of high angular momentum pair formation relative to the non-mixing case. Landau level mixing acts to inhibit Laughlin correlations relative to the isolated Landau level models.

Our results for Landau level mixing in the first excited Landau level disagree with the results of a recent paper that calculated the effect of LL mixing on the pseudopotential using perturbation theory [Bishara and Nayak (2009)]. Their perturbation results predict that LL mixing should have a much smaller effect than our results suggest. In addition, our results predict that Landau level mixing should act to always depress the pseudopotential, while their results predict a slightly positive change in the pseudopotential for odd values of R. It is unsurprising that the

perturbation results would disagree with our exact numerical diagonalization results because, at experimentally typical magnetic fields, the parameter $\kappa(B)$ is on the order of 1, suggesting that Landau level mixing is too strong to be considered a small perturbation to the system.

It should be reasonable to use the Landau level mixing affected pseudopotentials presented to modify numerical systems with n-electrons confined to a single Landau level in order to predict how Landau level mixing affects the behavior of condensed states in the quantum Hall system. An additional aspect of Landau level mixing that is not addressed is known as level crowding. In a nearly filled Landau level, the presence of so many electrons highly restricts the available wavefunctions for electronic transitions. As such, a electrons in a highly crowded LL may be more easily excited to higher LLs than electrons in a less crowded system. However, we believe the effect of Landau level crowding may not be very strong. Although transitions from the highly crowded Landau level to a higher, empty Landau level may be encouraged by level crowding, the same level crowding will simultaneously act to discourage excitations from lower, filled Landau levels. Because the two-particle matrix elements of section 2.3 are typically of the same order for single Landau level transitions (transitions from the n^{th} to the $(n+1)^{st}$ LL), we suspect that level crowding may not alter the predicted Landau level mixing pseudopotential significantly.

Chapter 5

Conclusions

In this dissertation, I have evaluated new analytic expressions for the two-particle matrix elements and calculated the effect of Landau level mixing for the quantum Hall effect.

The analytic expressions extend the work of [G. Fano (1986)] from the lowest Landau level, LL0, into all higher Landau levels. The new expressions also rewrite the quantum Hall problem in terms of the well-understood field of angular momentum algebra. In addition, they simplify the calculation of the two-body matrix elements and improve modeling techniques by connecting the pair pseudopotential $V(L)$ more directly to the inter-electron spatial potential, $V(r_{ij})$. Using our expressions, we have run some preliminary simulations indicating that well-width effects in the quantum Hall effect are very small if the width is smaller than the magnetic length, in agreement with the results of [Peterson et al. (2008)].

My calculations of the effect of Landau level mixing indicate that Landau level mixing is very weak in LL0, but the effect is more significant in the first excited Landau level, LL1. The effect of Landau level mixing in LL1 becomes more important as the magnetic field strength is lowered enough that the Coulomb energy scale becomes comparable to or larger than $\hbar\omega_c$. Landau level mixing in LL1 decreases the pseudopotential $V(L)$ more strongly for the highest allowed values of the pair

angular momentum, L (corresponding to the lowest values of the relative angular momentum, $R = 2l - L$), and that decrease is most dramatic for the maximum pair angular momentum (which corresponds to $R = 1$ for spin-aligned fermions). As a result, we predict that Landau level mixing should suppress Laughlin correlations in the first excited Landau level; for samples in which $\kappa(B) = e^2/\hbar\omega_c 4\pi\epsilon\lambda$ is sufficiently large, the effect may be strong enough to disrupt some weak incompressible quantum liquid states in LL1.

The calculations on the effect of Landau level mixing should be useful in various future studies as a parameter for improving theoretical models of the system. It will be useful to see how Landau level mixing affects the correlations and energy gaps in LL1 incompressible quantum liquid states. The LL mixing results should be included in numerical models used to calculate quasiparticle pseudopotentials formed from states in LL1. Future studies incorporating Landau level mixing might indicate systems in which the effects of changes in $\kappa(B)$ could be experimentally observed. Finally, we would like to apply our results to composite fermion quasiparticles in studies of the novel incompressible quantum liquid states observed experimentally [Pan et al. (2003)].

Bibliography

Bibliography

Ashcroft, N. and Mermin, N. (1976). *Solid State Physics*. Thomas Learning, Inc., United States. 2

Bethe, H. A. and Jackiw, R. (1986). *Intermediate Quantum Mechanics*. The Benjamin/Cummings Publishing Company, Menlo Park, California. 52

Bishara, W. and Nayak, C. (2009). Effect of landau level mixing on the effective interaction between electrons in the fractional quantum hall regime. *Phys. Rev. B*, 80:121302. 72, 82

Dev, G. and Jain, J. K. (1992). Band structure of the fractional quantum hall effect. *Phys. Rev. Lett.*, 69:2843–2846. 8

Edmonds, A. R. (1996). *Angular Momentum in Quantum Mechanics*. Princeton University Press, Princeton, New Jersey. 21, 22, 23, 24, 25, 27, 28, 38, 48, 54

Eisenstein, J. P. and Stormer, H. L. (1990). The fractional quantum hall effect. *Science, New Series*, 248:1510–1516. 3

Friedrich, H. (2006). *Theoretical Atomic Physics*. Springer, Berlin, Germany. 52

G. Fano, F. Ortolani, E. C. (1986). Configuration-interaction calculations on the fractional quantum hall effect. *Phys. Rev. B*, 34:2670. 13, 30, 84

Goldman, V. J. and Su, B. (1995). Resonant Tunneling in the Quantum Hall Regime: Measurement of Fractional Charge. *Science*, 267:1010–1012. 5

Haldane, F. D. M. (1983). Fractional quantization of the hall effect: A hierarchy of incompressible quantum fluid states. *Phys. Rev. Lett.*, 51:605–608. 5, 9, 58

Hassitt, A. (1955). Fractional parentage coefficients and their explicit evaluation. *Proc. R. Soc. Lond. A*, 229:110–119. 47

Haynes, W. M., editor (2011-2012). *CRC Handbook of Chemistry and Physics, 92nd edition*. CRC Press/Taylor and Francis, Boca Raton, FL. 71

Jain, J. K. (1989). Composite-fermion approach for the fractional quantum hall effect. *Phys. Rev. Lett.*, 63:199–202. 6, 58

Kivelson, S., Kallin, C., Arovas, D. P., and Schrieffer, J. R. (1987). Cooperative ring exchange and the fractional quantum hall effect. *Phys. Rev. B*, 36:1620. 30, 32

Klitzing, K. V., Dorda, G., and Pepper, M. (1980). New Method for High-Accuracy Determination of the Fine-Structure Constant Based on Quantized Hall Resistance. *Physical Review Letters*, 45:494–497. 2

Landau, L. D. and Lifshitz, E. M. (1965). *Quantum Mechanics Non-relativistic Theory*. Pergamon Press, Oxford, England. 3

Laughlin, R. B. (1983). Anomalous quantum hall effect: An incompressible quantum fluid with fractionally charged excitations. *Phys. Rev. Lett.*, 50:1395–1398. 4, 8

Moore, G. and Read, N. (1991). Nonabelions in the fractional quantum hall effect. *Nuclear Physics B*, 360(2-3):362 – 396. 8

Morf, R. H., d'Ambrumenil, N., and Das Sarma, S. (2002). Excitation gaps in fractional quantum hall states: An exact diagonalization study. *Phys. Rev. B*, 66:075408. 72

Nayak, C., Simon, S. H., Stern, A., Freedman, M., and Das Sarma, S. (2008). Non-abelian anyons and topological quantum computation. *Rev. Mod. Phys.*, 80:1083–1159. 10

NIST (2005). Codata recommended values of the fundamental physical constants: 2002 @ONLINE. 2

Pan, W., Stormer, H. L., Tsui, D. C., Pfeiffer, L. N., Baldwin, K. W., and West, K. W. (2003). Fractional quantum hall effect of composite fermions. *Phys. Rev. Lett.*, 90:016801. 12, 13, 85

Peterson, M. R., Jolicoeur, T., and Das Sarma, S. (2008). Orbital landau level dependence of the fractional quantum hall effect in quasi-two-dimensional electron layers: Finite-thickness effects. *Phys. Rev. B*, 78:155308. 36, 84

Prange, R. E. and Girvin, S. M. (1987). *The Quantum Hall Effect*. Springer-Verlag, New York. 11, 30

Quinn, J. and Wójs, A. (2000). Composite fermions and the fractional quantum hall effect: essential role of the pseudopotential. *Physica E: Low-dimensional Systems and Nanostructures*, 6(1-4):1 – 4. 12

Simon, S. H., Rezayi, E. H., and Cooper, N. R. (2007). Pseudopotentials for multiparticle interactions in the quantum hall regime. *Phys. Rev. B*, 75:195306. 11

Sitko, P., Yi, S. N., Yi, K. S., and Quinn, J. J. (1996). "fermi liquid" shell model approach to composite fermion excitation spectra in fractional quantum hall states. *Phys. Rev. Lett.*, 76:3396–3399. 12

Tsui, D. C., Stormer, H. L., and Gossard, A. C. (1982). Two-dimensional magnetotransport in the extreme quantum limit. *Phys. Rev. Lett.*, 48:1559–1562. 2

U. Fano, G. R. (1959). *Irreducible Tensorial Sets*. Academic Press, New York. 47, 62

Wójs, A. and Quinn, J. J. (1998). Composite fermion approach to the quantum hall hierarchy: when it works and why. *Solid State Communications*, 108(7):493 – 497. 12

Wójs, A. and Quinn, J. J. (2000). Quasiparticle interactions in fractional quantum hall systems: Justification of different hierarchy schemes. *Phys. Rev. B*, 61:2846–2854. 40, 61

Wójs, A. and Quinn, J. J. (2006). Landau level mixing in the $\nu = 5?2$ fractional quantum hall state. *Phys. Rev. B*, 74:235319. 72

Wu, T. T. and Yang, C. N. (1976). Dirac monopole without strings: Monopole harmonics. *Nuclear Physics B*, 107(3):365 – 380. 20, 23, 27

Wu, T. T. and Yang, C. N. (1977). Some properties of monopole harmonics. *Phys. Rev. D*, 16:1018–1021. 20, 21, 25

Yi, K. and Quinn, J. (1997). Fermi liquid shell model descriptions of composite fermions. *Solid State Communications*, 102(11):775 – 777. 12

Yoshioka, D. (1984). Effect of landau level mixing on the ground state of two-dimensional electrons. *J. Phys. Soc. Jpn.*, 53:3740–3743. 72, 74

Yoshioka, D. (2002). *The Quantum Hall Effect*. Springer, Berlin, Germany. 33

Vita

Rachel Wooten was born in Oak Ridge, TN to Doctor John Wooten and Dianne Wooten. After graduating from Oak Ridge High School in 2002, she attended Vanderbilt University in Nashville, TN from 2002 until 2006, when she graduated with a Bachelor's of Science with a double major of Physics and Mathematics and a minor in Chemistry. She then attended the University of Tennessee, Knoxville and studied theoretical condensed matter physics with Dr. Joseph Macek and Dr. John Quinn. She obtained a Doctorate of Philosophy in Physics in the spring of 2013.